

Toward an ab Initio Derivation of Crystal Morphology

Ziva Berkovitch-Yellin

Contribution from the Department of Structural Chemistry, The Weizmann Institute of Science, Rehovot, 76100 Israel. Received December 5, 1984

Abstract: A method is presented for the calculation of the habit of organic crystals from known crystal structure and symmetry. Calculated morphologies are found to be in good agreement with observations for crystals grown by sublimation. To obtain the habit of solution-grown crystals solvent/solute interactions at the crystal/solution interface must be considered. It was assumed that the solvent affects the habit of crystals through preferential adsorption of solvent molecules on specific crystal faces; the need to remove the solvation layer prior to the deposition of oncoming crystal layers causes retardation of growth of these faces relative to their growth rate from the vapor. Changing the relative growth rates of the various faces leads to a change in crystal shape. Electrostatic potential maps at closest approach distances were used for the study of the relative polarities of the various crystal faces, information which is crucial for the prediction of the habits of crystals obtained from solution in polar or nonpolar solvents.

1. Introduction

The shape of a crystal is determined by the relative rates of deposition of particles on its various faces, the general rule being that faces which grow slowest appear as large developed faces. The growth rates are determined primarily by the strength of binding of the particles which arrive at the several crystal surfaces, and this depends on the internal architecture of the crystal. However, any factor which may cause an alteration in the rate of deposition at any surface will influence the crystal habit. External factors which may do so are temperature, supersaturation, solvent, and impurity concentration.

The relation between the morphology of a crystal and its internal structure and symmetry, at a molecular level, attracted the attention of scientists long before the internal structure could be determined from diffraction data. However, due to its complexity, the derivation of crystal morphology still remained a basic problem in the theory of crystal growth.

Recently we have systematically studied the effect of additives on crystal growth and shape.¹⁻⁵ It was observed that small amounts of "tailor-made" growth retarders, which are slightly modified substrate molecules, if added to the solution of crystallizing material, have a dramatic effect on the shape of deposited crystals. To understand the mechanism of the effect of additives sufficiently well to permit their systematic use to induce preselected modifications of crystal habit, we have studied the relationship between crystal structure and morphology and the systematics of the interactions between a crystallizing substrate and its environment in general, and the solvent and stereospecific "tailor-made" additives in particular.

In the early literature, the morphology of a crystal, represented by the "morphological importance" (M.I.)⁶ of its various faces, was derived from the interplanar distance d_{hkl} ,⁷ corrected for the extinction conditions of the space group,⁸ according to the rule that the larger d_{hkl} the more pronounced is the M.I. of the face. Later the periodic bond chain (PBC) theory of Hartman and

Perdok provided a tool for the calculation of the M.I. of crystal faces.⁹ In this method the various faces are classified as F (flat), S (stepped), or K (kinked) according to the number of periodic bond chains which are found in the plane parallel to the face (at least two, one, or none for F, S, and K faces, respectively). They proposed that the attachment energy (E_{att}), defined as the energy per molecule released when a new layer is attached to the surface of the crystal, is a measure of the growth rate (R) normal to a face, so that faces with higher E_{att} grow faster and have lower M.I. Thus, for faces f_1 and f_2 , if $|E_{att1}| > |E_{att2}|$ then $R_1 > R_2$ and $M.I._1 < M.I._2$. In most cases F faces are those with the largest M.I.

An important factor which may affect the shape of crystals is the exact mechanism of growth. According to current theories the growth of a flat crystal face (F face) proceeds layer after layer. For an ideal crystal, a new layer is initiated by two-dimensional nucleation; for a real crystal, a screw dislocation emerging at the surface permits the perpetual exposure of a layer edge, which serves as a nucleation site for the initiation of a new layer.¹⁰ Hartman and Bennema¹¹ analyzed the role played by E_{att} in controlling the growth and shape of crystals growing according to various growth mechanisms. They demonstrated that for crystals growing at low supersaturations, the simple relation $R_{rel} \propto E_{att}$ (R_{rel} is the relative growth rate of the face) is a valid approximation and may be used for the derivation of growth forms of crystals. Several calculations of crystal morphology based on this assumption have been published and are in nice agreement with observed forms.¹² In some cases in which the calculated and observed forms differ, the discrepancies were accounted for by assuming solvent¹³ or impurity effects.¹⁴

Calculated crystal habits derived from the internal structure are best compared with those of crystals obtained by sublimation. For solution-grown crystals the effect of interactions between solute and solvent molecules at the various crystal/solution interfaces may have a pronounced influence on the shape of the crystal. Habit modifications due to solvent were first described by Wells,¹⁵ who explained the observed effects as due to preferential adsorption

(1) Addadi, L.; Berkovitch-Yellin, Z.; Domb, N.; Gati, E.; Lahav, M.; Leiserowitz, L. *Nature (London)* **1982**, *296*, 21-26.

(2) Berkovitch-Yellin, Z.; Addadi, L.; Idelson, M.; Leiserowitz, L.; Lahav, M. *Nature (London)* **1982**, *296*, 27.

(3) Berkovitch-Yellin, Z.; Addadi, L.; Idelson, M.; Lahav, M.; Leiserowitz, L. *Angew. Chem. Suppl.* **1982**, 1336.

(4) Addadi, L.; Berkovitch-Yellin, Z.; Weissbuch, I.; Lahav, M.; Leiserowitz, L. *Mol. Cryst. Liq. Cryst.* **1983**, *96*, 1-17.

(5) Berkovitch-Yellin, Z.; Van Mil, J.; Addadi, L.; Idelson, M.; Lahav, M.; Leiserowitz, L. *J. Am. Chem. Soc.* **1985**, *107*, 3111-3122.

(6) The M.I. is a statistical quantity which describes the relative frequency of occurrence and the size of a crystal face in a crop of crystals. The higher the M.I. of a face, the larger is its size and the higher the frequency of its occurrence.

(7) Friedel, G. *Bull. Soc. Fr. Mineral.* **1907**, *30*, 326.

(8) (a) Donnay, J. D. H.; Harker, D. *Am. Mineral.* **1937**, *22*, 446. (b) Donnay, J. D. H.; Donnay, G. *C. R. Acad. Sci. Paris* **1961**, *252*, 908.

(9) (a) Hartman, P.; Perdok, W. G. *Acta Crystallogr.* **1955**, *8*, 49-52. (b) Hartman, P.; Perdok, W. G. *Ibid.* **1955**, *8*, 521-524. (c) Hartman, P.; Perdok, W. G. *Ibid.* **1955**, *8*, 525-529. (d) Hartman, P. In "Crystal Growth: An Introduction"; Hartman, P. Ed.; North Holland: Amsterdam, 1975; p 367.

(10) Frank, F. C. *Discuss. Faraday Soc.* **1949**, *5*, 48.

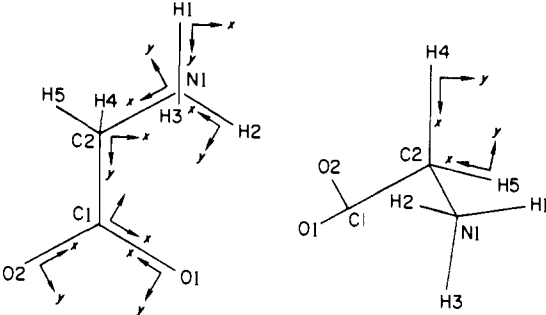
(11) Hartman, P.; Bennema, P. *J. Cryst. Growth* **1980**, *49*, 145-156.

(12) (a) Hartman, P. *J. Cryst. Growth* **1980**, *49*, 157-165. (b) Hamer, R.; Tassoni, D.; Riquet, J. P.; Durand, F. *Ibid.* **1981**, *51*, 493-501. (c) Tassoni, D.; Riquet, J. P.; Durand, F. *Acta Crystallogr., Sect. A* **1980**, *36*, 420-428.

(13) (a) Saska, M.; Myerson, A. S. *J. Cryst. Growth* **1983**, *61*, 546-555. (b) Human, H. J.; Van der Eerden, J. P.; Jetten, L. A. M. J.; Odekerken, G. M. *Ibid.* **1981**, *51*, 589-600.

(14) (a) Hartman, P. *J. Cryst. Growth* **1980**, *49*, 166-170. (b) Visser, R. A.; Bennema, P. *Neth. Milk Dairy J.* **1983**, *37*, 109-137.

(15) Wells, A. F. *Philos. Mag.* **1946**, *37*, 184.

Table I. Electrostatic Properties of Glycine: Net Atomic Charges (q , e), ($\times 10^4$) dipole (d , $e \text{ \AA}$), and Second Moments (μ , $e \text{ \AA}^2$) ($\times 10^4$) in Local Coordination Systems x , y , z Centered on Each Atom^a


atom	charge ^a (e), q	dipole moment, ^a $e \text{ \AA}$			second moment, ^a $e \text{ \AA}^2$					
		d_x	d_y	d_z	μ_{xx}	μ_{yy}	μ_{zz}	μ_{xy}	μ_{yz}	μ_{xz}
N1	-680	78	173	17	389	450	527	54	-4	1
O1	-1726	25	446	43	-246	-366	-181	-151	-6	-1
O2	-3002	287	26	98	-432	-73	-454	108	-32	-33
C1	146	149	-78	5	-201	-191	706	-109	22	32
C2	-736	-638	250	-12	308	436	643	36	29	13
H2	1323	-301	5	-2	105	305	293	-3	-9	-3
H2	1155	-276	-25	-34	54	246	253	12	-26	-21
H3	1215	-312	51	14	83	270	237	12	-4	29
H4	1109	-585	3	41	195	327	292	15	46	17
H5	1197	-662	25	-56	273	334	327	9	-36	24

^a The net atomic charge for an atom i , $q_i = \int \delta\rho_i(\mathbf{r}) d\mathbf{v}$, where $\delta\rho_i(\mathbf{r})$ is the atom deformation density and \mathbf{r} is measured from the nucleus of atom i ; the negative sign obeys the convention that electrons are negatively charged. The atomic dipole moment $d_{i,x} = -\int x_i \delta\rho_i(\mathbf{r}) d\mathbf{v}$, where x is the component of the vector \mathbf{r} . Similar expressions apply to $d_{i,y}$ and $d_{i,z}$. The second moment tensor of $\delta\rho_i(\mathbf{r})$ has six components $\mu_{i,xx}$, $\mu_{i,yy}$, $\mu_{i,zz}$, etc. $\mu_{i,xy} = -\int xy \delta\rho_i(\mathbf{r}) d\mathbf{v}$.

of solvent molecules on specific faces, with a concomitant delay in the growth rate of these faces. Other examples of solvent effect on crystal morphology have appeared in the literature.¹⁶ In these publications, the effect of solvent was explained in an alternative manner by its effect on the surface perfection and growth mechanism.

Growth rates and crystal habit are appreciably changed by specific adsorption of impurities at mole fractions as low as 10^{-9} M. The modification of crystal habit by impurities may originate from two opposite effects: adsorption of impurities at kinks, steps, or ledge sites may cause inhibition of growth.^{17a} However, impurities with strong bonds to the host lattice may afford centers of enhanced nucleation and so produce a large increase in the growth rate.^{17b}

The study of the effect of impurities on crystal growth and shape was simplified by the use of "tailor-made" additives. Due to the close resemblance in molecular structure between the substrate and these additives, the interactions between them at the various substrate crystal faces are very stereospecific and relatively easy to model. Systematic studies have led to the formulation of a two-step mechanism of adsorption and inhibition of growth.¹ The highly predictable effect of specific "tailor-made" additives has been exploited for the solution of various stereochemical problems.^{2-5,18}

In this paper, we describe the atom-atom potential-energy calculation of the intermolecular interactions in organic crystals and their use for the derivation of crystal morphology. In the next sections, we describe a method for the derivation of crystal habit from the internal structure and then outline models for predicting

the effects of solvent and of "tailor-made" additives.

2. Computational Details

2.1. Interatomic Potential Functions. The energy functions used in the calculations included van der Waals and electrostatic terms. The first term was described by a Lennard-Jones (6-9) potential, with parameters derived by Hagler et al. for polar molecules,¹⁹ slightly modified by fit our different description of the electrostatic term which included interactions between net atomic charges, dipoles, and quadrupole moments placed at the atomic positions. The electrostatic parameters were derived from deformation electron density maps obtained from low-temperature X-ray diffraction data.²⁰ The parameters used for the energy calculations of various amide and carboxylic acid derivatives have been published elsewhere;^{21,22} those for glycine (Table I) were derived from an experimental deformation density distribution of crystalline α -glycine²⁵ derived from low-temperature diffraction data. Potential functions of this type have been successfully applied to the analysis of packing characteristics.²¹⁻²⁴

2.2. Calculation of Layer Energy and Attachment Energy. We have calculated the intermolecular interactions between a reference molecule and all the other molecules in the crystal. The sum of these interactions defines the crystal energy (E_{cr}) which is twice the sublimation energy (E_{sub}) of the crystal.²⁶ The summation limit was determined by increasing the size of the crystal until there was no significant change in E_{cr} on incorporating more molecules in the summation. These intermolecular interactions were used for the calculation of the attachment energy (E_{att}) and layer energy (E_l) of various low-index crystal faces. The latter

(16) (a) Davey, R. J. In "Current Topics in Material Science"; Kaladis, E., Ed.; North-Holland: Amsterdam, 1982; Chapter 6. (b) Bourne, J. R.; Davey, R. J. *J. Cryst. Growth* **1976**, *36*, 278-286. (c) Skoda, W.; Van den Tempel, M. *Ibid.* **1967**, *1*, 207-217. (d) Bourne, J. R.; Davey, R. J. *Ibid.* **1978**, *43*, 224-228. (e) Davey, R. J.; Mullin, J. W.; Whiting, M. J. L. *Ibid.* **1982**, *58*, 304-312.

(17) (a) Davey, R. J. *J. Cryst. Growth* **1976**, *34*, 109-119. (b) Gilmer, G. H. *Science* **1980**, *208*, 355-363.

(18) (a) Addadi, L.; Berkovitch-Yellin, Z.; Weissbuch, I.; Lahav, M.; Leiserowitz, L.; Weinstein, S. *J. Am. Chem. Soc.* **1982**, *104*, 2075-2077. (b) Weissbuch, I.; Berkovitch-Yellin, Z.; Addadi, L.; Lahav, M.; Leiserowitz, L. *Isr. J. Chem.* **1985**, *25*, 353-361. (c) Weissbuch, I.; Addadi, L.; Berkovitch-Yellin, Z.; Gati, E.; Weinstein, S.; Lahav, M.; Leiserowitz, L. *J. Am. Chem. Soc.* **1983**, *105*, 6615-6621.

(19) (a) Hagler, A. T.; Huler, E.; Lifson, S. *J. Am. Chem. Soc.* **1974**, *96*, 5319-5327. (b) Lifson, S.; Hagler, A. T.; Dauber, P. *Ibid.* **1979**, *101*, 5111-5121.

(20) Hirshfeld, F. L. *Theor. Chim. Acta* **1977**, *44*, 226.

(21) Berkovitch-Yellin, Z.; Leiserowitz, L. *J. Am. Chem. Soc.* **1980**, *102*, 7677-7690.

(22) Berkovitch-Yellin, Z.; Leiserowitz, L. *J. Am. Chem. Soc.* **1982**, *104*, 4052-4064.

(23) Berkovitch-Yellin, Z.; Ariel, S.; Leiserowitz, L. *J. Am. Chem. Soc.* **1983**, *105*, 765-767.

(24) Berkovitch-Yellin, Z.; Leiserowitz, L. *Acta Crystallogr., Sect. B* **1984**, *40*, 159-165.

(25) Legros, J. P.; Kvik, A. *Acta Crystallogr., Sect. B* **1980**, *36*, 3052-3059.

(26) Busing, W. R. *J. Phys. Chem. Solids* **1978**, *39*, 691.

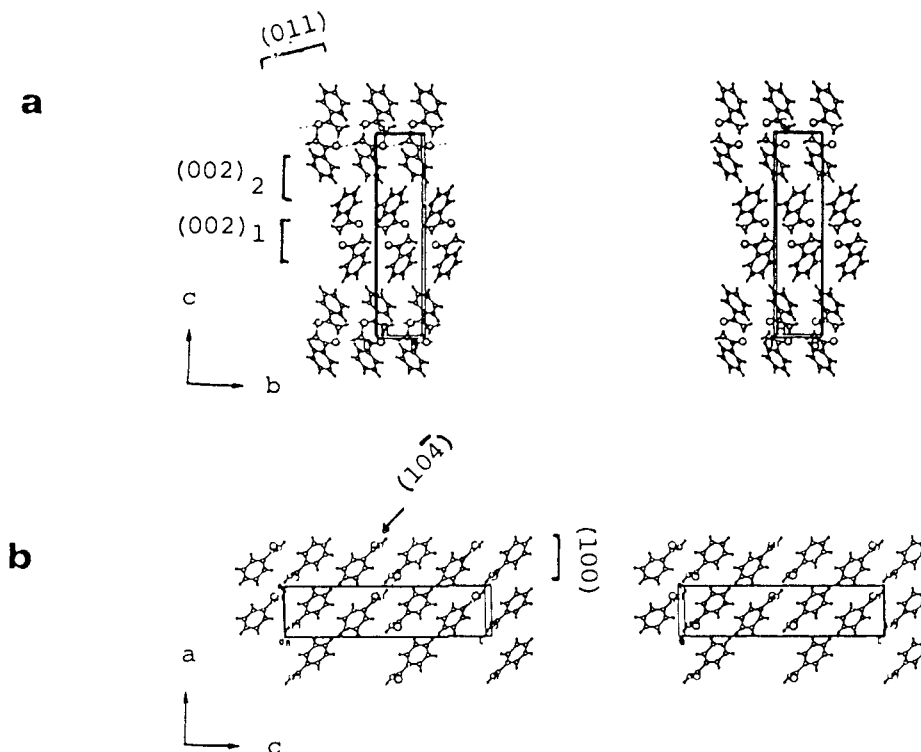


Figure 1. Packing arrangement of benzamide as viewed (a) along the *a* axis, (b) along the *b* axis. "Edge-on" views of some layers are indicated.

Table II. Benzamide: Strongest Intermolecular Interactions (kcal/mol) in the Crystal^a

neighbor ^b			symmetry	<i>E</i>	<i>U</i>	<i>E</i> + <i>U</i>
site						
<i>a</i> ₁	<i>a</i> ₂	<i>a</i> ₃				
0	1	0	1	-5.87	-4.24	-10.10
0	-1	0	1			
2	0	0	3	-10.38	-1.85	-12.23
1	0	0	3	-4.48	-4.79	-9.26
1	-1	-1	2	-0.56	-2.60	-3.16
1	0	-1	2			
-1	-1	1	1	-1.27	-1.23	-2.50

^a *E* = electrostatic energy; *U* = van der Waals energy. ^b The site of the neighboring molecule is described by the lattice vector $V = a_1a + a_2b + a_3c$ and the space group symmetry operator. *a*, *b*, and *c* are the unit cell dimension. ^c (1) *x*, *y*, *z*, (2) $-x$, $1/2 + y$, $1/2 - z$; (3) $-x$, $-y$, $-z$; (4) x , $1/2 - y$, $1/2 + z$.

Table III. Benzamide: Layer Energy (*E*_l, kcal/mol) and Attachment Energy (*E*_{att}, kcal/mol) of Various Low-Index Faces

face	<i>E</i> _l	<i>E</i> _{att}	face	<i>E</i> _l	<i>E</i> _{att}
(002) ₁ ^{a,b}	-52.45	-6.00	{10 $\bar{6}$ }	-31.20	-16.63
(002) ₂ ^{a,b}	-42.62	-10.93	{102}	-30.63	-16.91
{10 $\bar{2}$ }\subscript{1} ^b	-38.67	-12.91	{20 $\bar{2}$ }\subscript{a}	-29.79	-17.33
{100}	-37.34	-13.59	{202}\subscript{a}	-28.82	-17.82
{10 $\bar{4}$ }	-33.85	-15.30	{020}\subscript{a}	-26.29	-19.08
{004}\subscript{c}	-33.51	-15.47	{1 $\bar{1}$ 1}	-16.47	-23.99
{102}\subscript{2} ^b	-32.66	-16.39	{111}	-11.88	-26.29
{011}	-31.62	-16.42			

^a Halving of some layers is done because of space group symmetry *P*2₁/*c*. ^b There are two alternative ways to define this layer. ^c A natural sublayer of spacing $1/2d_{hkl}$. *E*_l and *E*_{att} for this layer were calculated similarly to the other layers.

is defined⁹ as the energy per molecule released when a layer is formed. The layer (*hkl*) is defined by the vector (*S*_{*hkl*}) perpendicular to the plane *hkl*

$$S_{hkl} = ha^* + kb^* + lc^* = \mathbf{n}_{hkl}(1/d_{hkl})$$

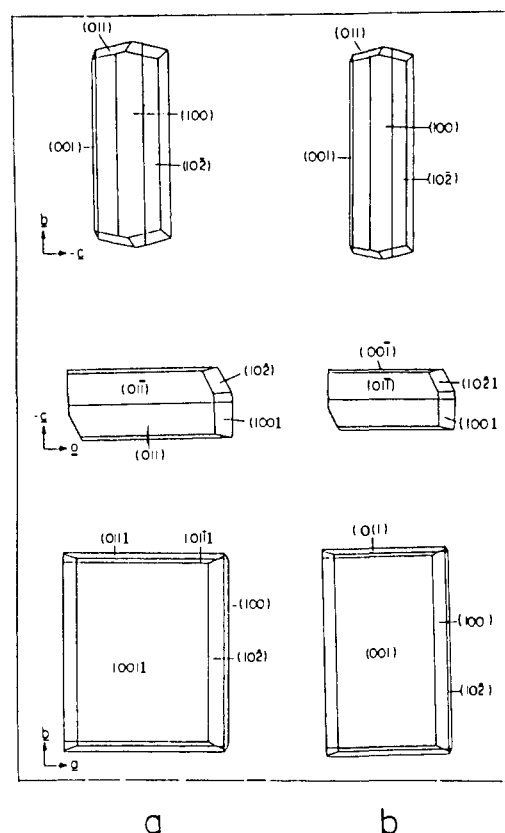


Figure 2. Computer-drawn pictures of benzamide crystals as viewed along the *a*, *b*, and *c* axes (i, ii, and iii, respectively): (a) the "theoretical form"; (b) crystals obtained by sublimation.

where *a*^{*}, *b*^{*}, and *c*^{*} are the reciprocal cell dimensions, *n*_{*hkl*} is a unit vector, and *d*_{*hkl*} is the interplanar spacing of the plane *hkl*, taking submultiples due to lattice centering or to screw axes or glide planes perpendicular to the plane, i.e., (002) or (020) instead of (001) or (010), respectively.²⁷ *E*_l is calculated as the sum of

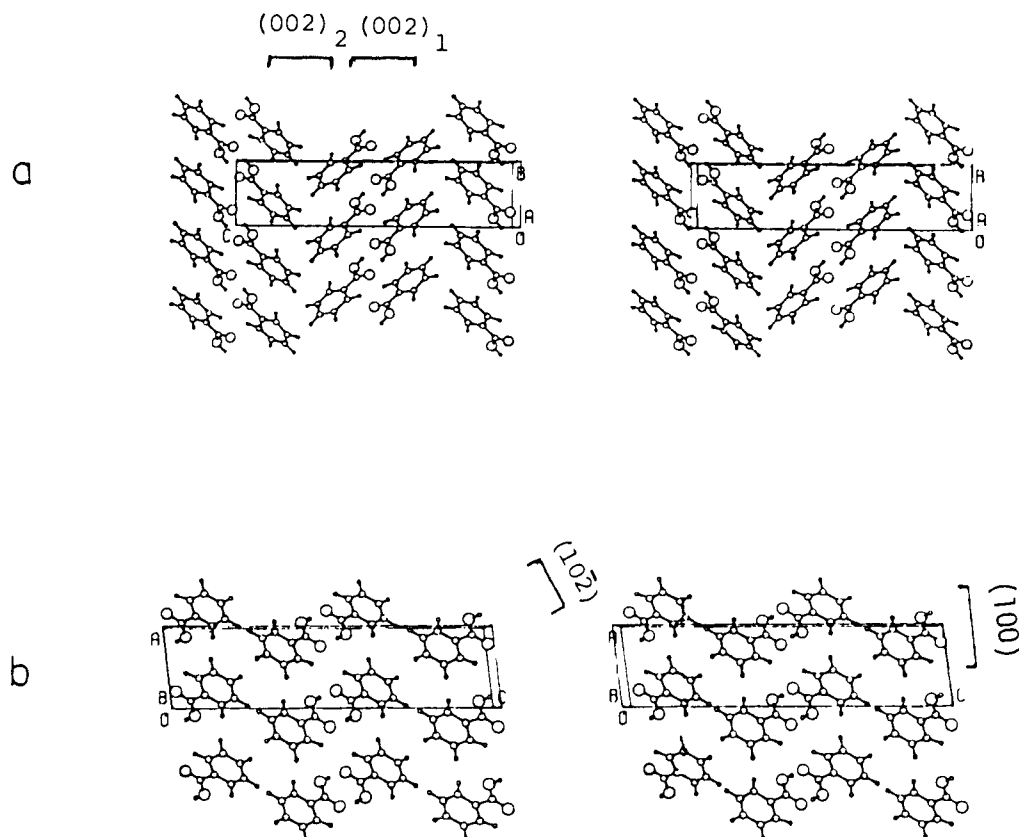


Figure 3. Packing arrangement of benzoic acid as viewed (a) along the a axis; (b) along the b axis. "Edge-on" views of some layers are indicated.

Table IV. Benzoic Acid: Strongest Intermolecular Interactions (kcal/mol) in the Crystal^a

neighbor ^b			symmetry	E	U	$E + U$
site						
a_1	a_2	a_3				
0	0	0	2	-3.98	-3.25	-7.23
0	-1	0	1	-0.52	-5.60	-6.12
0	1	0	1			
0	1	0	2	0.27	-5.08	-4.81
1	0	0	1	-0.29	-3.43	-3.72
1	0	0	1			
1	-1	0	3	-0.10	-1.87	-1.97
1	0	0	3			
1	1	0	2	-0.15	-1.70	1.85
0	0	0	3	0.00	-1.61	-1.61
0	-1	0	3			
-1	-1	0	1	-0.16	-1.12	-1.28
1	1	0	1			

^a E = electrostatic energy; U = van der Waals energy. ^bSee Table II.

Table V. Benzoic Acid: Layer Energy (E_1 , kcal/mol) and Attachment Energy (E_{att} , kcal/mol) of Various Low-Index Faces Arranged in Decreasing Order of Their E_1

face	E_1	E_{att}	face	E_1	E_{att}
{002} ₁ ^{a,b}	-39.86	-4.94	{011}	-19.10	-15.32
{002} ₂ ^{a,b}	-32.28	-8.73	{202} ^a	-16.03	-16.85
{104}	-25.62	-12.06	{104}	-15.64	-17.05
{102}	-29.82	-9.96	{111}	-11.42	-19.16
{100}	-29.26	-10.24	{111}	-11.08	-19.33
{202} ^a	-25.17	-12.28	{110}	-9.58	-20.08
{004} ^c	-23.72	-13.01			
{102}	-19.11	-15.31			

^{a-c}See Table III.

all intermolecular interactions between a reference molecule and its neighbors within the layer of width d_{hkl} . The molecules belonging to the layer satisfy the condition:

$$|\mathbf{r}_j \cdot \mathbf{n}_{hkl}| < d_{hkl}/2$$

\mathbf{r}_j is the vector from the center of gravity of molecule j to that of a reference molecule (1) at the center of the layer. E_{att} is computed by summing all intermolecular interactions between the reference molecule and all molecules outside the layer (hkl) in one-half of the crystal (at the negative direction of \mathbf{S}_{hkl}). Thus, the vector \mathbf{r}_j between the reference molecule and each of the molecules, the interaction of which are summed up to yield E_{att} , satisfy the condition

$$(\mathbf{r}_j \cdot \mathbf{n}_{hkl}) < -d_{hkl}/2$$

E_1 and E_{att} of each layer are not independent quantities; the crystal energy is equal to

$$E_{cr} = E_1(hkl) + E_{att}(hkl) + E_{att}(\bar{h}\bar{k}\bar{l})$$

For pure crystals, neglecting interactions with the environment (solvent, impurities) or polarizability, $E_{att}(hkl) = E_{att}(\bar{h}\bar{k}\bar{l})$

$$E_{cr} = E_1 + 2E_{att}$$

therefore

$$E_{sub} = \frac{1}{2}E_1 + E_{att} = \text{constant}^{28}$$

E_{sub} is the sublimation energy, which may be obtained from experimental data. To eliminate the possibility of dependence of E_1 and E_{att} of various faces on the choice of the reference molecule, the calculation of these properties was repeated n_s times (n_s being the number of unique molecules in the unit cell). Thus, the reference molecule was placed in turn at each of the general

(27) A screw axis (2_1) or a glide plane halves the interplanar distance of a face perpendicular to it because the same surface configuration is repeated after a period $\frac{1}{2}d_{hkl}$.

(28) By definition our E_1 is half E_{sl} defined by Hartman, while E_{att} is the same as his.⁹

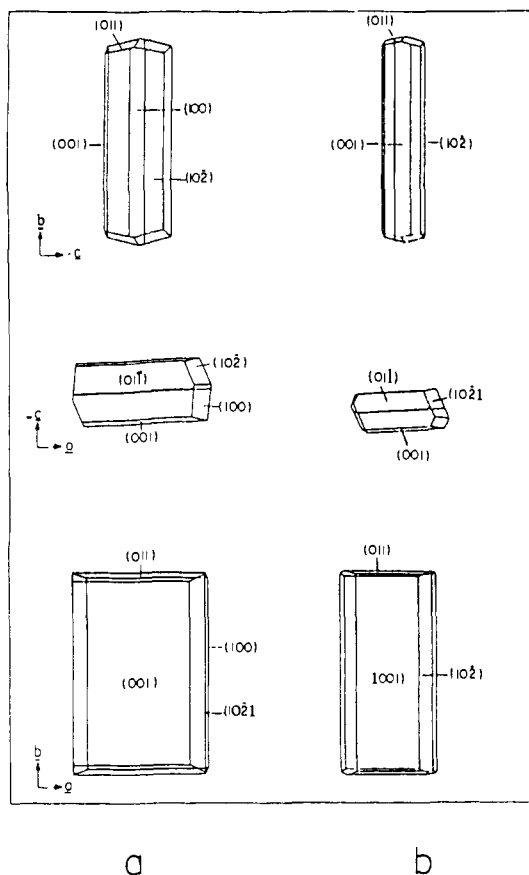


Figure 4. Computer-drawn pictures of benzoic acid crystals as viewed along the *a*, *b*, and *c* axes (i, ii, and iii, respectively): (a) the "theoretical form"; (b) crystals obtained by sublimation.

positions of the unit cell. In the calculation of the pure crystal, E_1 and E_{att} were obtained by averaging the respective values obtained in each of the n_s calculations. In the calculations of the habit in the presence of additives no averaging was done, as differences between the sites on various faces are significant.^{5,18}

In some cases the layer is not uniquely defined and two layers (with E_{11} and E_{12}) are possible. To check for such possibility the calculation of E_1 of each layer is repeated with the origin shifted from the center of gravity of the reference molecule by $\pm 0.5 \text{ \AA}$ along the vector S_{hkl} and the calculated E_1 compared with that derived with the center of gravity of the reference molecule at the center of the layer. If $E_{11} \approx E_{12}$ (and thus $E_{att1} \approx E_{att2}$) the two layers are of similar stability and both layers grow simultaneously; thus we took the growth rate as proportional to the average E_{att} of both layers (which is, in fact, very close to each value separately). However, if one layer is distinctly more stable than the other, i.e., $|E_{11}|$ is much larger than $|E_{12}|$, growth is controlled by the more stable layer which grows much slower than the alternative layer;²⁹ thus we took E_{att1} as representing the growth rate normal to this face. In some cases there are in the crystal natural layers of width $1/2 d_{hkl}$, i.e., (040) instead of (020) or (004) instead of (002). Hartman and Heijnen^{29a} make a distinction between cases where the sublayer has an F character or not. So if $E_{11} = E_{12}$ and the layer $1/2 d_{hkl}$ is of type F, growth will be determined by E_1 of this half-layer. If the layer $1/2 d_{hkl}$ is of S or K character, growth will occur by layers d_{hkl} but will be enhanced through nucleation at the half-step edge.

In the calculation of E_1 the structure of the layer (hkl) was taken to be identical with that of a similar layer in the bulk of the crystal, so by assuming that these layers represent the surface layers, or the elementary growth units, distortions at the interface are not

considered. Entropy effects are also neglected and thus the calculation is most accurate at 0 K.

From the values of E_1 and E_{att} of various low-index faces, it is possible to predict the faces of the crystal³⁰ and its habit, as decreasing $|E_{att}|$ implies an increase in the M.I. of the face. The stable faces, for which $|E_1| > |E_{att}|$, are the real and virtual faces³¹ of the crystal. The latter are defined as stable faces which may become real faces once their growth rate is somewhat decreased. This can be due to any external factor such as interaction with solvent or with impurity.

2.3. The "Theoretical Form". The polyhedron which is delimited by the most stable faces (which grow the slowest) is denoted the "theoretical form" of the crystal. The "theoretical form" is derived from the relative growth rates (R_{rel}) of various low-index faces. The latter are represented by E_{att} using the relation

$$R \propto E_{att}$$

and

$$R_{rel} = R_i/R_j = E_{att_i}/E_{att_j}$$

Here *i* and *j* are two crystal faces of which *j*, usually the most stable face, is chosen as a reference.

The habits are derived from the relative growth rates of the stable faces in a procedure which is similar to a Wulff construction.³² From a chosen origin we draw normals to all possible faces of length proportional to the corresponding R_{rel} . A plane is drawn through the end of each normal and perpendicular to it. The polyhedron enclosed by these planes represents the "theoretical form" of the crystal.

2.4. Modelling the Effect of Solvent on Crystal Habit. We assumed that the main effect of the solvent originates from preferential adsorption of solvent molecules on specific crystal faces (see discussion). The need to remove the solvation layer prior to the deposition of the next layer causes a delay in growth of these faces relative to other faces and to their growth rate from the vapor. Such a delay may induce a change in crystal habit. Assuming further that polar solvents preferentially interact with polar faces and nonpolar solvents with nonpolar faces, a large solvent effect is anticipated for crystals exhibiting faces with large differences in polarity. The polarity of a face is determined by the atoms which are exposed normal to the face and are easily accessed by solvent molecules. To establish the polarity of the various crystal faces we analyzed their structure and mapped the electrostatic potentials along the various surface layers. The potential was calculated on a grid that followed the surface contour at closest approach distance. The perpendicular distance of each grid point from the surface layer (the elevation) was chosen so that the minimal distance of approach to any atom of the surface layer is 2.6 Å. These maps represent the energy released when ions or polar molecules are at close contact and interact with the molecules of the surface layer. The relative polarity of the faces was deduced from these electrostatic potential maps by various statistical analyses³³ performed on the positive and negative potential values separately. All the tests yielded similar results as to the relative polarities of the various crystal faces. We chose to present here the root mean square (rms) of the positive and negative potential values as a measure of this property.

2.5. Modelling the Effect of "Tailor-Made" Additives. It has been established¹⁻³ that "tailor-made" impurities, which are slightly modified substrate molecules, when added during crystallization, selectively replace a substrate molecule at the host crystal sites only on those faces where the modified part of the additive emerges

(30) It is noteworthy that in cases where there is not a strong anisotropy in the crystal, namely, there is not an extremely strong intermolecular interaction at a specific direction, the faces which are calculated to be the most stable faces (with the most negative E_1) are F faces, those with the least negative E_1 are the K faces. Thus, it is possible from the energy values to choose the F faces with no need to perform a detailed PBC⁹ analysis.

(31) Johnson, A. "Wachstum und Auflösung der Kristalle"; Wilh. Engelmann, Leipzig, 1900.

(32) Wulff, G. Z. *Kristallogr.* **1901**, *34*, 449.

(33) Spiegel, M. R. "Statistics", Schaum Outline Series; McGraw-Hill: New York, 1961; Chapters 2 and 3.

(29) (a) Hartman, P.; Heijnen, W. M. M. *J. Cryst. Growth* **1983**, *63*, 261-264. (b) Bennema, P.; Giess, E. A.; Weidenborner, J. E. *Ibid.* **1983**, *62*, 41-60.

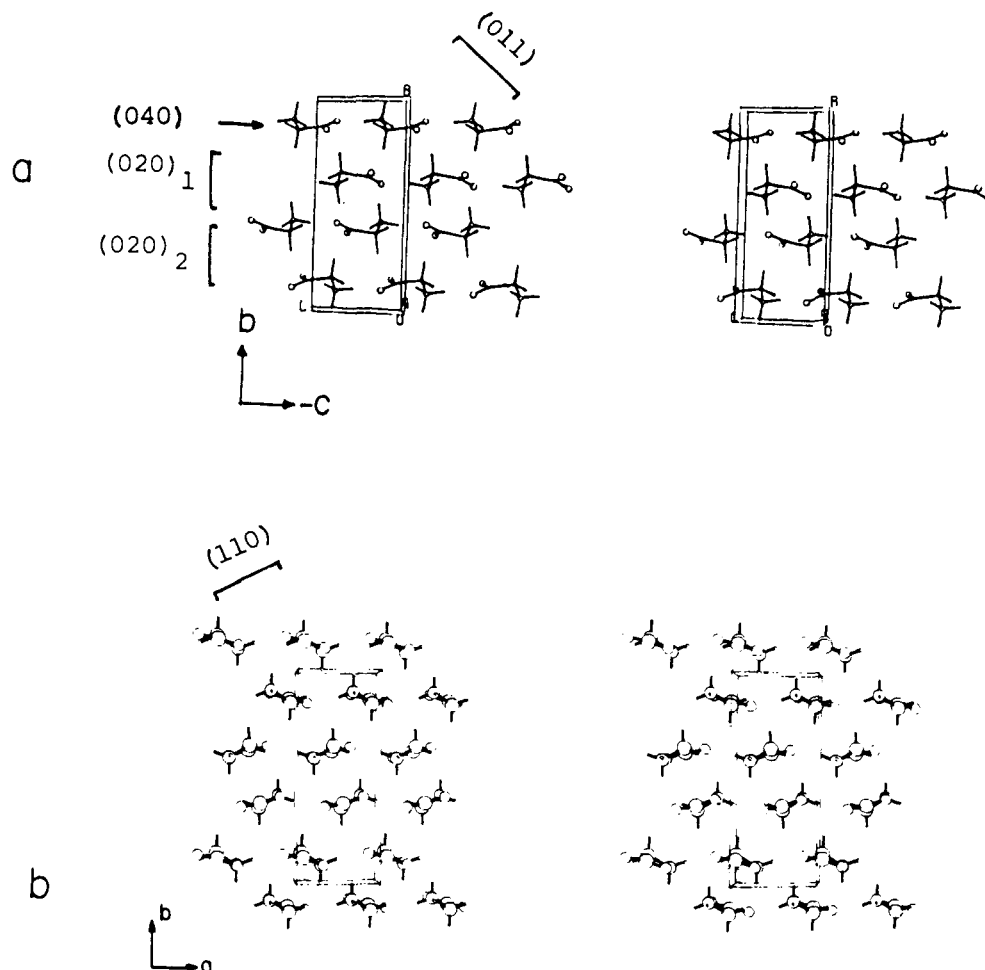


Figure 5. Packing arrangement of α -glycine as viewed (a) along the a axis; (b) along the c axis. "Edge-on" views of some layers are indicated.

Table VI. α -Glycine: Strongest Intermolecular Interactions (kcal/mol) in the Crystal^a

neighbor ^b			symmetry ^c	E	U	$E + U$
site						
a_1	a_2	a_3				
0	0	0	3	-10.60	-2.57	-13.16
0	0	-1	1	-6.85	-0.74	-7.56
0	0	1	1			
1	0	0	3	-6.43	-0.59	-7.02
-1	0	0	2	-3.08	-0.13	-3.21
0	0	-1	2			
-1	0	1	1	-2.27	-0.19	-2.46
1	0	-1	1			
-1	-1	-1	4	-2.14	-0.27	-2.41
-1	1	-1	4			
-1	0	-1	3	-2.13	-0.27	-2.39
0	0	0	4	-1.44	-0.36	-1.80
0	-1	0	4			
-1	0	1	2	-0.92	-0.42	-1.35
1	1	-2	2			
-1	0	1	3	2.19	-0.48	1.71
1	0	-1	3	2.80	-0.44	2.36
0	0	0	2	5.25	-1.50	3.75
-1	0	-1	2			

^a E = electrostatic energy, U = van der Waals energy. ^b See Table II. ^c (1) x, y, z ; (2) $1/2 + x, 1/2 - y, 1/2 + z$; (3) $-x, -y, -z$; (4) $1/2 - x, 1/2 + y, 1/2 - z$.

Table VII. α -Glycine: Layer Energy (E_l , kcal/mol) and Attachment Energy (E_{att} , kcal/mol) of Various Low-Index Faces Arranged in Decreasing Order of Their E_l

face	E_l	E_{att}	face	E_l	E_{att}
(020) ₁ ^{a,b}	-40.37	-6.47	{10 $\bar{1}$ }	-31.00	-11.15
{110}	-35.26	-9.02	{011}	-27.34	-12.98
{002} ^a	-32.18	-10.56	(020) ₂ ^{a,b}	-27.30	-13.00
{200} ^a	-32.00	-10.65	{101}	-24.03	-14.64
			{040} ^c	-23.9	-14.70

^a Halving of some layers is done because of space group symmetry $P2_1/n$. ^{b,c} See Table III.

from the crystal surface. The additive is bound in a very similar way to the substrate molecules by virtue of interactions between its unmodified part and the neighboring substrate molecules in the layer. Once adsorbed the modified part of the adsorbate molecule inhibits the deposition of on-coming substrate layers, changing the relative growth rates of the faces thus inducing morphological modifications which are generally an increase in the M.I. of the faces on which it is adsorbed. To establish these faces we look for those faces on which the additive replaces a substrate molecule with a minimal loss in binding energy. We calculated differences in binding energy of specific additives relative to substrate molecules, at each of the crystallographic sites on various crystal faces. The binding energy at a surface site is defined as $E_b = E_l + E_{att}$ for a substrate molecule, and $E'_b = E'_l + E'_{att}$ for the impurity, where E'_l and E'_{att} are the layer and attachment energies for a single impurity in a substrate crystal.

In the calculations it was assumed that the part of the additive identical with the substrate adopts a conformation similar to that of the substrate molecule. When the additive is a rigid molecule, its conformation is uniquely defined by the conformation of its

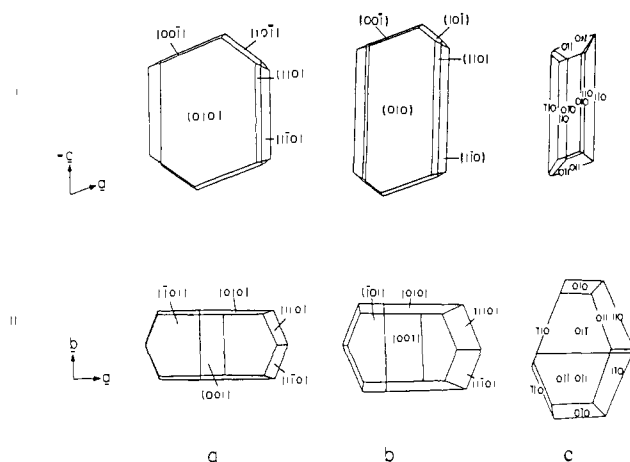


Figure 6. Computer-drawn pictures of α -glycine crystals as viewed along the b and c axes (i and ii, respectively): (a) the "theoretical form"; (b) crystals obtained by sublimation; (c) crystals obtained from aqueous solution.

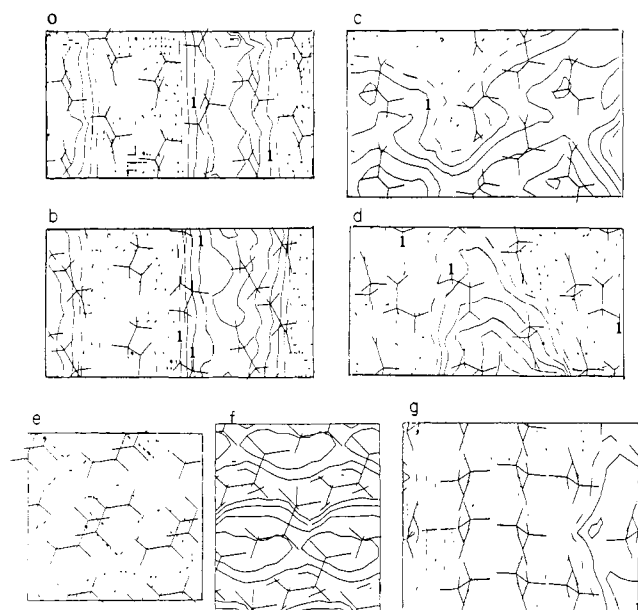


Figure 7. Electrostatic potential maps at closest approach distance to various faces of α -glycine. Molecules belonging to the surface layers are projected on the potential maps. Solid lines represent repulsive and dotted lines attractive interactions. Contour interval for (a-d) is 5 kcal/mol for (e,f) 2 kcal/mol, and for (g) 10 kcal/mol. The rms values (in kcal/mol) of the negative and positive potential values are given in parentheses: (a) $\{001\}$ (-28.8, 16.4); (b) $\{011\}$ (-29.2, 13.5); (c) $\{100\}$ (-9.6, 12.7); (d) $\{110\}$ (-15.5, 14.2); (e) $(020)_1$ (-5.2, 1.1); (f) $(020)_2$ (-2.7, 4.2); (g) $\{101\}$ (-53.8, 13.5).

unmodified part. When the modified part is a flexible molecular fragment, it may, in principle, adopt various conformations. However, we have found that the conformation of this part of the additive is also uniquely determined by the highly stereospecific intermolecular interactions between the adsorbed additive and the neighboring molecules in the crystal surfaces at which it is bound.³⁴

The derivation of the "theoretical forms" of various organic crystals is described in next sections. These are compared with observed habits of crystals grown by sublimation; then the effect of the solvent is introduced. The results of a detailed analysis, both experimental and theoretical, of the effect of "tailor-made" additives are presented in separate papers.^{5,18,34}

3. Results

3.1. Benzamide crystallizes from ethanol in space group $P2_1/c$, ($a = 5.61$, $b = 5.05$, $c = 22.05$ Å; $\beta = 90.7^\circ$) as rectangular (001) plates extended in b . In benzamide crystal³⁵ hydrogen-bonded

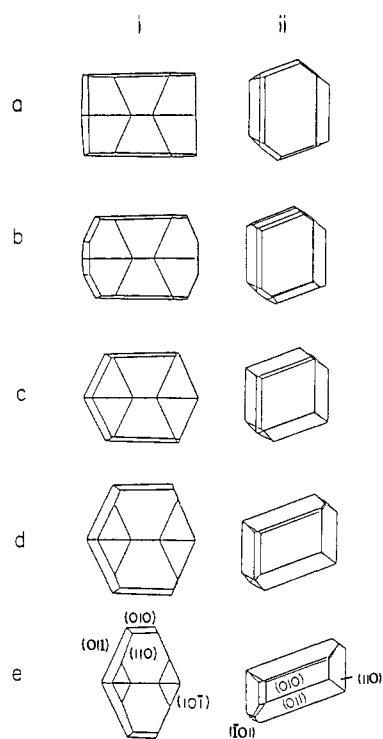


Figure 8. Simulation of the effect of polar solvent on the habit of α -glycine crystals. The gradual change in habit as function of (a) a decrease of E_{att} of all faces, but (010) by 30%, (b-e) a further decrease in the growth rate of $\{011\}$, by decreasing E_{att} in steps of 2 kcal/mol; (a) as viewed along the a axis; (b) as viewed along the b axis.

cyclic dimers are interlinked along the b axis to form H-bonded ribbons (Figure 1a) which are stacked along the a axis (Figure 1b). The ribbon and stack motifs combine to yield stable 001 layers. These tightly packed layers juxtapose along the c axis by weaker van der Waals contacts between phenyl groups (Figure 1a,b).

The calculated values for the strongest intermolecular interactions between a reference benzamide molecule and 310 neighboring molecules in the crystal are presented in Table II. The calculated E_1 and E_{att} of various low-index faces are listed in Table III in decreasing order of their M.I. There are two alternative ways to define the (002) (Figure 1a) and $(10\bar{2})$ layers. $(002)_1$ is distinctly more stable than $(002)_2$ (Table III), and therefore $E_{att,1}$ was chosen to represent the growth rate of the (001) face. For similar reasons $E_{att}(10\bar{2})_1$ was chosen to represent the growth rate of $(10\bar{2})$. The "theoretical form", derived from the calculated E_{att} , is in nice agreement with observed benzamide crystals obtained by sublimation (Figure 2).

3.2. Benzoic acid crystallizes from petroleum ether/hexane, in space group $P2_1/c$ ($a = 5.52$, $b = 5.14$, $c = 21.90$ Å; $\beta = 97.0^\circ$) in the form of bars extended along b . In the crystal³⁶ benzoic acid molecules form almost coplanar hydrogen-bonded dimers which are stacked in ribbons along b (Figure 3a), held together by $\text{CH}\cdots\text{O}$ interactions (Figure 3b). These combined ribbon and stack motifs generate 001 layers.

The calculated values for the strongest intermolecular interactions between a reference benzoic acid molecule and 380 neighbors in the crystal are presented in Table IV. The calculated E_1 and E_{att} of various low-index faces are listed in Table V in decreasing order of their M.I. The "theoretical form" derived from the calculated E_{att} is in nice agreement with observed benzoic acid crystals obtained by sublimation (Figure 4).

(34) Weissbuch, I.; Berkovitch-Yellin, Z.; Lahav, M.; Leiserowitz, L.; *Isr. J. Chem.* **1985**, *25*, 362-372.

(35) Blake, C. C. F.; Small, R. W. H. *Acta Crystallogr. Sect. B* **1972**, *28*, 2201.

(36) Sim, G. A.; Robertson, J. M.; Goodwin, T. H. *Acta Crystallogr.* **1955**, *8*, 157-164.

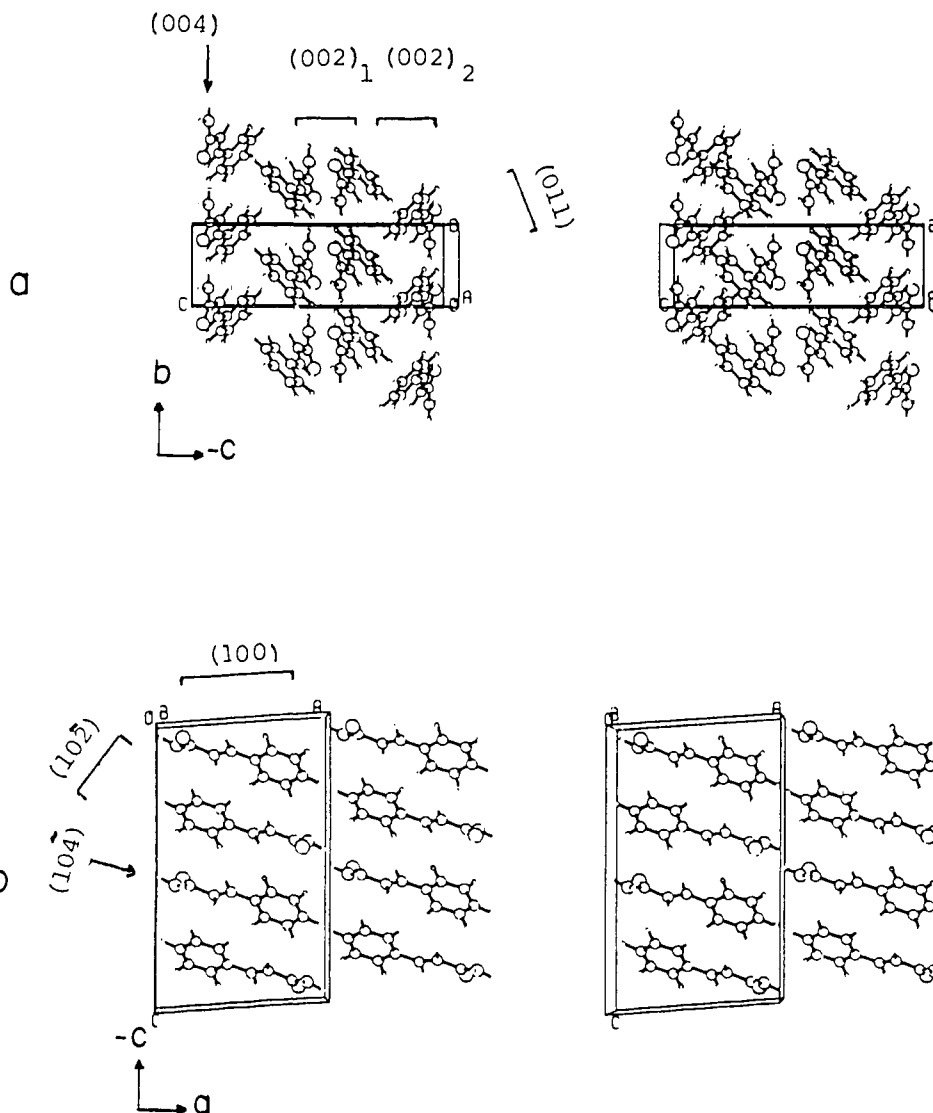


Figure 9. Packing arrangement of (*E*)-cinnamide as viewed (a) along the *a* axis; (b) along the *b* axis. "Edge-on" views of some layers are indicated.

Table VIII. (*E*)-Cinnamide: Strongest Intermolecular Interactions (kcal/mol) in the Crystal^a

neighbor ^b			symmetry ^c	<i>E</i>	<i>U</i>	<i>E</i> + <i>U</i>
site						
<i>a</i> ₁	<i>a</i> ₂	<i>a</i> ₃				
2	1	1	3	-10.06	-1.69	-11.75
0	-1	0	1	-6.19	-5.04	-11.24
0	1	0	1			
1	-1	0	2	-0.66	-6.12	-6.78
1	0	0	2			
1	1	1	3	2.23	-8.58	-6.35
1	0	1	3	-0.80	-2.89	-3.69
1	0	0	1	-0.56	-2.00	-2.56
-1	0	0	1			
0	0	0	2	0.20	-1.37	-1.17
0	-1	0	2			
1	0	1	3	-0.76	-0.89	-1.65
2	2	1	3	2.09	-0.43	1.66

^a *E* = electrostatic energy; *U* = van der Waals energy. ^b See Table II. ^c (1) *x*, *y*, *z*; (2) *-x*, $\frac{1}{2} + y$, $\frac{1}{2} - z$; (3) *-x*, *-y*, *-z*; (4) *x*, $\frac{1}{2} - y$, $\frac{1}{2} + z$.

3.3. α -Glycine. The stable, α -form of glycine is obtained from aqueous solution, in a monoclinic space group $P2_1/n$ ($a = 5.08$,

Table IX. (*E*)-Cinnamide: Layer Energy (*E*₁, kcal/mol) and Attachment Energy (*E*_{att}, kcal/mol) of Various Low-Index Faces Arranged in Decreasing Order of Their *E*₁

face	<i>E</i> ₁	<i>E</i> _{att}	face	<i>E</i> ₁	<i>E</i> _{att}
{100}	-53.80	-10.43	{10 $\bar{4}$ }	-35.68	-19.49
(002) ₁ ^{a,b}	-51.53	-11.56	{011}	-33.04	-20.81
(002) ₂ ^{a,b}	-47.83	-13.42	{004} ^c	-29.87	-22.39
{10 $\bar{2}$ }	-50.18	-12.24	{104}	-25.29	-24.68
{202} ^a	-39.21	-17.72	{020} ^a	-23.76	-25.45
{102}	-36.57	-12.24	{110}	-15.55	-29.56
{202} ^a	-36.04	-19.31			

^{a-c} See Table III.

$b = 11.82$, $c = 5.46$ Å; $\beta = 112^\circ$). In the crystal of glycine²⁵ the molecules form hydrogen-bonded layers parallel to the *ac* plane. Each layer is interlinked to its neighbors by NH \cdots O hydrogen bonds and by CH \cdots O contacts to form stable (020) bilayers (Figure 5). α -Glycine crystals obtained from aqueous solution are bipyramidal with $2/m$ morphological symmetry (Figure 6c).³⁷ The M.I. of the various faces derived from their surface areas and frequency of occurrence are:

$$\text{M.I.}\{011\} = \text{M.I.}\{110\} \gg \text{M.I.}\{010\}^{38}$$

(37) α -Glycine crystals obtained from aqueous solution are bipyramidal in shape. In some cases the base of the pyramid is elongated along the *a* axis and in other cases along the *c* direction (Figure 6), depending on the experimental conditions (Weissbuch, I., private communication).

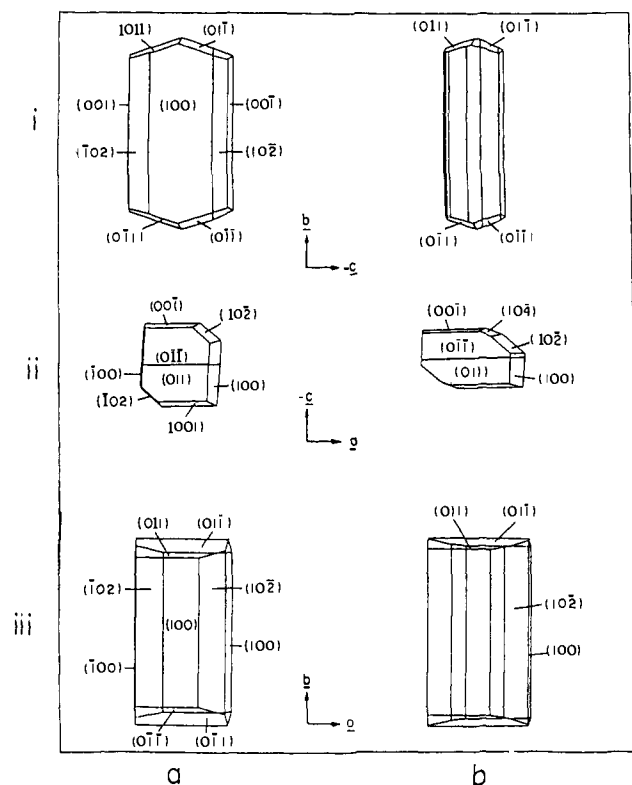


Figure 10. Computer-drawn pictures of (*E*)-cinnamide crystals as viewed along the *a*, *b*, and *c* axes (i, ii, and iii, respectively): (a) the "theoretical form"; (b) crystals obtained by sublimation.

The calculated values for the strongest intermolecular interactions between a reference glycine molecule and 360 neighbors in the crystal are presented in Table VI. The calculated E_1 and E_{att} of various low-index faces are listed in Table VII in decreasing order of their M.I.

There are two alternative ways to define the (020) layer (Figure 5a): one with $E_1 = -40.4$ kcal/mol and the other with $E_1 = -27.3$ kcal/mol. The first alternative is much more stable than the second, and thus E_{att1} (Table VII) was taken as representing the growth rate normal to {010}. The "theoretical form", which was derived from the calculated E_{att} , is shown in Figure 6a. The M.I. of the various faces of the "theoretical form", based on their surface areas, are:

$$\text{M.I.}\{010\} > \text{M.I.}\{001\} > \text{M.I.}\{110\} > \text{M.I.}\{10\bar{1}\}$$

The "theoretical form" of glycine is in very good agreement with the morphology of crystals obtained by sublimation³⁹ (Figure 6b), but it is distinctly different from that of α -glycine crystals grown from aqueous solution (Figure 6c). The most pronounced differences are the complete absence in the latter of {001} and {10 $\bar{1}$ }, the appearance of large {011}, and the drastic reduction in the area of {010}. In α -glycine crystal there is a natural (040) monolayer which may be considered as the growing unit of the {010} face, rather than the (020) bilayer, composed of glycine dimers strongly interlinked by NH \cdots O H bonds (Figure 5a), which is selected according to the space group conditions (section 2.2). However, when the "theoretical form" was drawn using $E_{att}(040)$ (Table VII) as representing the growth rate normal to {010}, the resulting habit was very different from that of α -glycine crystals obtained by sublimation. This may suggest that the "building-blocks" of the crystal in the *ac* plane are indeed dimers, and thus the preassociation of glycine molecules to form the dimers occurs

(38) The symbol {} indicates all symmetry-related faces; () indicates just the given face; i.e., {010} represents the faces (010) and (0 $\bar{1}$ 0).

(39) α -Glycine crystals were grown by sublimation overnight in a closed vacuum tube. The bottom of the tube containing glycine crystals was heated to 145 °C, and the upper part of the tube, where the crystals grew, was kept at a temperature of 105 °C.

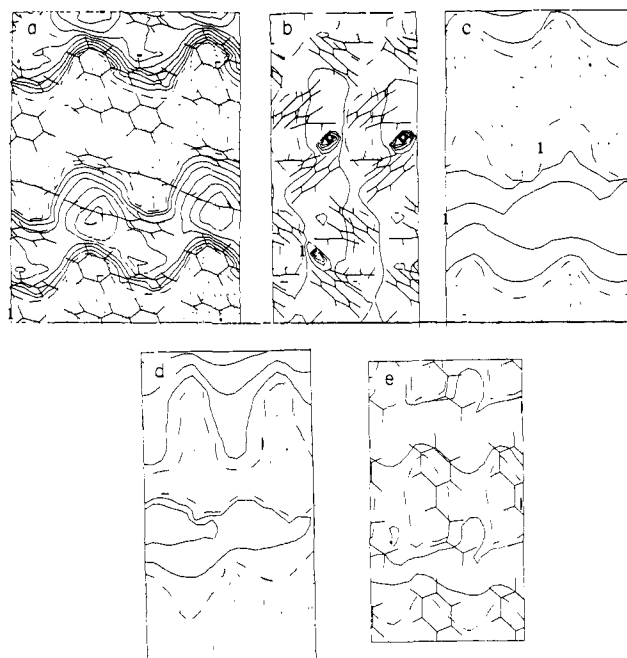


Figure 11. Electrostatic potential maps at closest approach distance to various faces of (*E*)-cinnamide. Molecules belonging to the surface layers are projected on some of the potential maps. Solid lines represent repulsive and dotted lines attractive interactions; contour interval 2 kcal/mol. The rms (in kcal/mol) of the negative and positive potential values are given in parentheses: (a) {011} (-12.3, 10.4); (b) {100} (-3.8, 3.9); (c) {10 $\bar{2}$ } (-4.4, 9.3); (d) {102} (-6.6, 4.0); and (e) {001} (-4.2, 2.8).

already in the gas phase. Indeed, intermolecularly hydrogen-bonded dimers of protonated and neutral α -amino acids were observed in high-pressure mass spectrometric measurements.⁴⁰

The large differences in habit between α -glycine crystals obtained by sublimation and those obtained from aqueous solution is attributed to a solvent effect (section 2.4).

To establish the relative polarities of the various faces of α -glycine, the electrostatic potentials at closest approach distance to these faces were mapped (Figure 7). From the maps and the rms values of the negative and positive potential values, it is clear that all layers are polar and thus will interact with polar solvents. Differences between the various polar faces arise from differences in their structure, such as different extents of exposure of the carboxylic oxygen atoms and of the NH $_3$ and hydrogen atoms. On the most polar faces, {011}, {001}, and {10 $\bar{1}$ } (Figure 7a,b,g), both oxygen atoms of the carboxyl group emerge normal to the face (Figure 5) and thus constitute good binding sites for polar solvent molecules like water. The CO $_2^-$ and NH $_3^+$ sites are represented in the electrostatic potential maps (Figure 7) by high negative and positive potential values, respectively. On the other hand, in the least polar face {010} (Figure 7e) the molecules lie in the *ac* plane, parallel to the face, and only CH hydrogen atoms emerge normal to the interface. Low positive potential values (<2 kcal/mol) are calculated at the sites where water molecules may bind to the face by CH \cdots O interactions, which are distinctly weaker than NH \cdots O H bonds.²⁴ The relatively low negative potential values, at the surface sites where H(water) \cdots O(glycine) H bonds are formed, result from an relatively unfavorable direction of approach of the donor water molecules toward the carboxyl group, from above the carboxyl plane.²² It is noteworthy that for a complete description of the effect of solvent on α -glycine crystals growing in aqueous solution, we must also consider an alternative structure of the interface between the crystal and solution at the {010} face, that in which NH atoms are exposed ((020) $_2$ or (040) layers, Figure 5a). The polarity of this interface (Figure 7f) is

(40) (a) Meot-Ner, M.; Field, F. H. *J. Am. Chem. Soc.* **1974**, *96*, 3168-3171. (b) Meot-Ner (Mautner), M.; Hunter, E. P.; Field, F. H. *Ibid.* **1979**, *101*, 686. (c) Gaffney, J. S.; Pierce, R. C.; Friedman, L. *Ibid.* **1977**, *99*, 4293-4298.

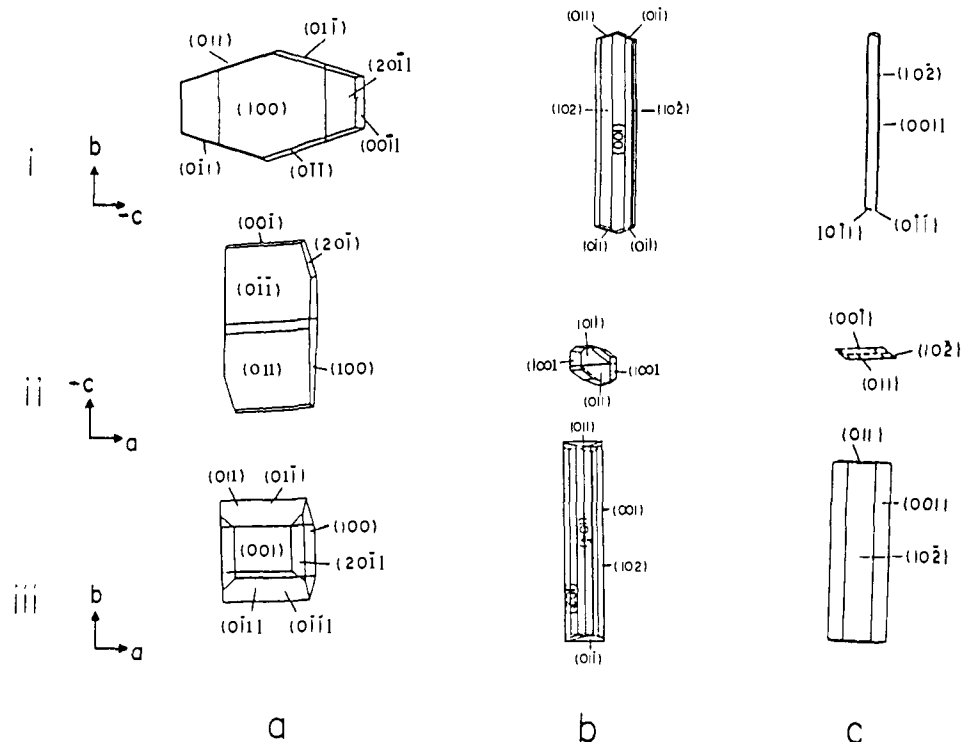


Figure 12. Computer-drawn pictures of (*E*)-cinnamide crystals obtained from solutions of various solvents, as viewed along the *a*, *b*, and *c* axes (i, ii, and iii, respectively): (a) from aqueous solution; (b) from ethyl acetate; (c) from benzene.

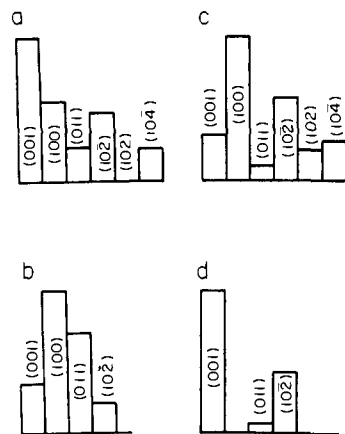


Figure 13. The M.I. of various faces of (*E*)-cinnamide crystals: (a) obtained by sublimation; (b) grown from aqueous solution; (c) grown from ethyl acetate; (d) grown from benzene.

comparable to that of the $(020)_1$ interface (Figure 7e) and is distinctly lower than the polarity of the other faces of α -glycine crystal. Consequently, the morphological modification induced by the polar water molecules on α -glycine crystal habit can be accounted for by assuming adsorption of solvent molecules on all faces but $\{010\}$ and preferentially on $\{011\}$.

To check this assumption we plotted the "theoretical form" of glycine with modified growth rates, represented by E_{att} . The growth rate of $\{010\}$ was kept unchanged; those of the other faces were decreased by an arbitrary factor of 30% to simulate a delay in growth rate (Figure 8a). The growth rate of $\{011\}$ was further reduced in a stepwise manner (by ΔE). Figure 8b–e presents the gradual change in habit of glycine crystals as a function of ΔE .

The resulting habit (Figure 8e) is in agreement with that of α -glycine crystals grown from aqueous solution³⁷ (Figure 6c) except for the small $\{101\}$ faces, which were never experimentally observed. We cannot explain, however, on these simple grounds, the observation that $\{001\}$ which are of large M.I. in crystals obtained from the vapor, are replaced by $\{011\}$ in α -glycine crystals obtained from aqueous solution, as both faces are of comparable

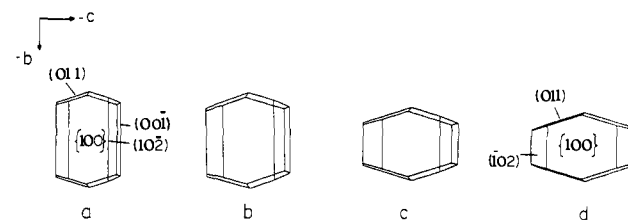


Figure 14. Simulation of the effect of polar solvent on the habit of (*E*)-cinnamide crystals: (a–d) The gradual change in habit as a result of decreasing the growth rate of $\{011\}$ by decreasing E_{att} in steps of 4 kcal/mol.

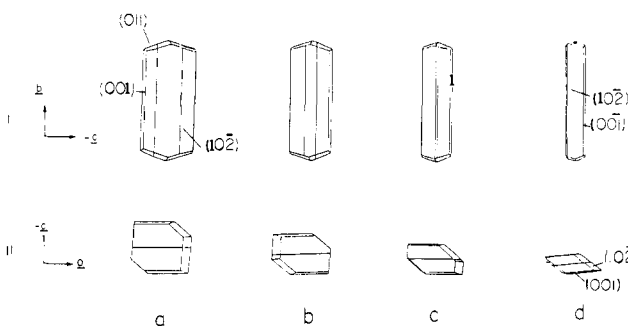


Figure 15. Simulation of the effect of nonpolar solvent on the habit of (*E*)-cinnamide crystals. The gradual change in habit as a result of decreasing the growth rate of $\{001\}$, by decreasing E_{att} in steps of 2 kcal/mol: (i) a view along the *a* axis; (ii) a view along the *b* axis.

polarities, and the absence of $\{10\bar{1}\}$ which are also polar faces. These questions may be resolved by a detailed calculation of the binding energy of the solvent molecules to these three surfaces, which may reveal a preference for water adsorption on the $\{011\}$ rather than $\{001\}$ and $\{10\bar{1}\}$. On the same basis, it is predicted that glycine crystals obtained from nonpolar solvents, e.g., benzene, will be (010) plates. This prediction could not be verified as glycine is insoluble in such solvents.

3.4. (*E*)-Cinnamide crystallizes in a monoclinic space group $P2_1/c$ ($a = 9.56$, $b = 5.14$, $c = 16.01$ Å; $\beta = 94.1^\circ$). In (*E*)-cinnamide crystals⁴¹ centrosymmetric dimers are interlinked by

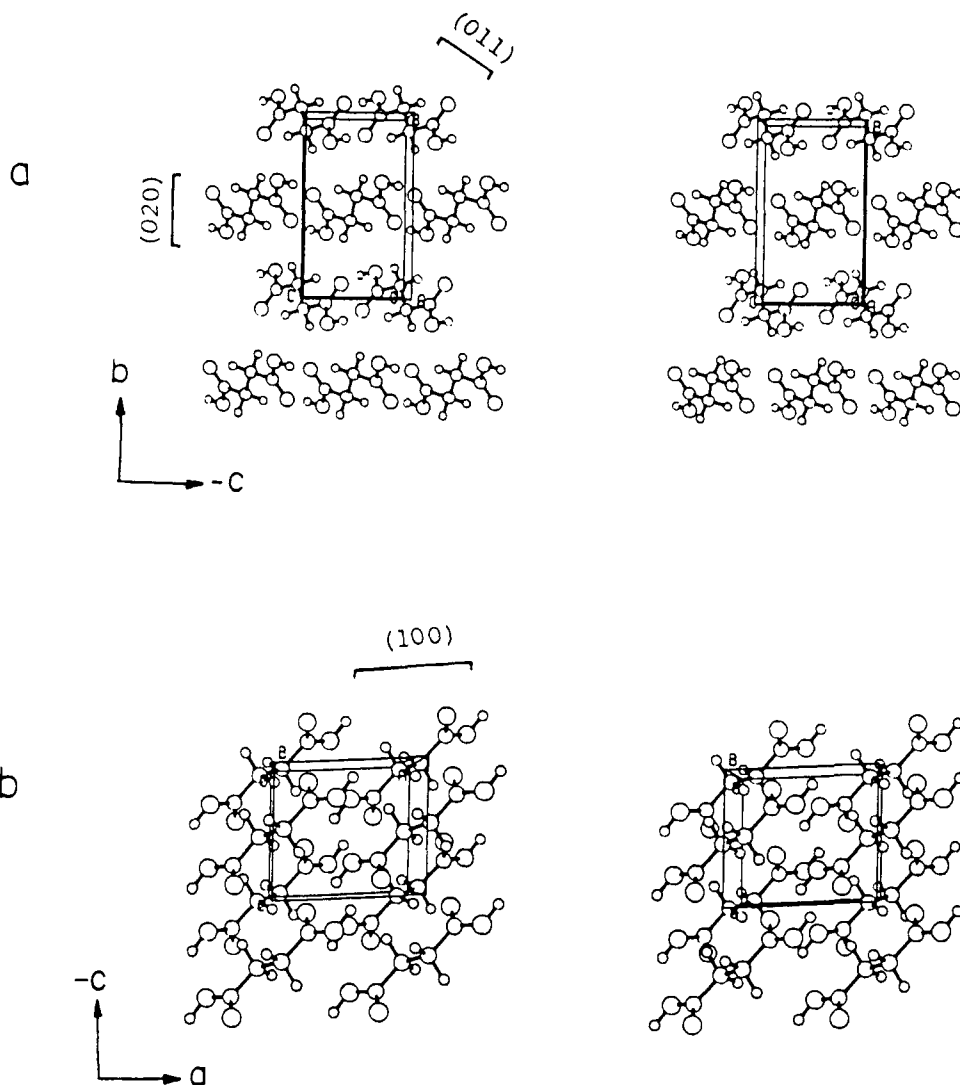


Figure 16. Packing arrangement of succinic acid viewed (a) along the *a* axis; (b) along the *b* axis. "Edge-on" views of some layers are indicated.

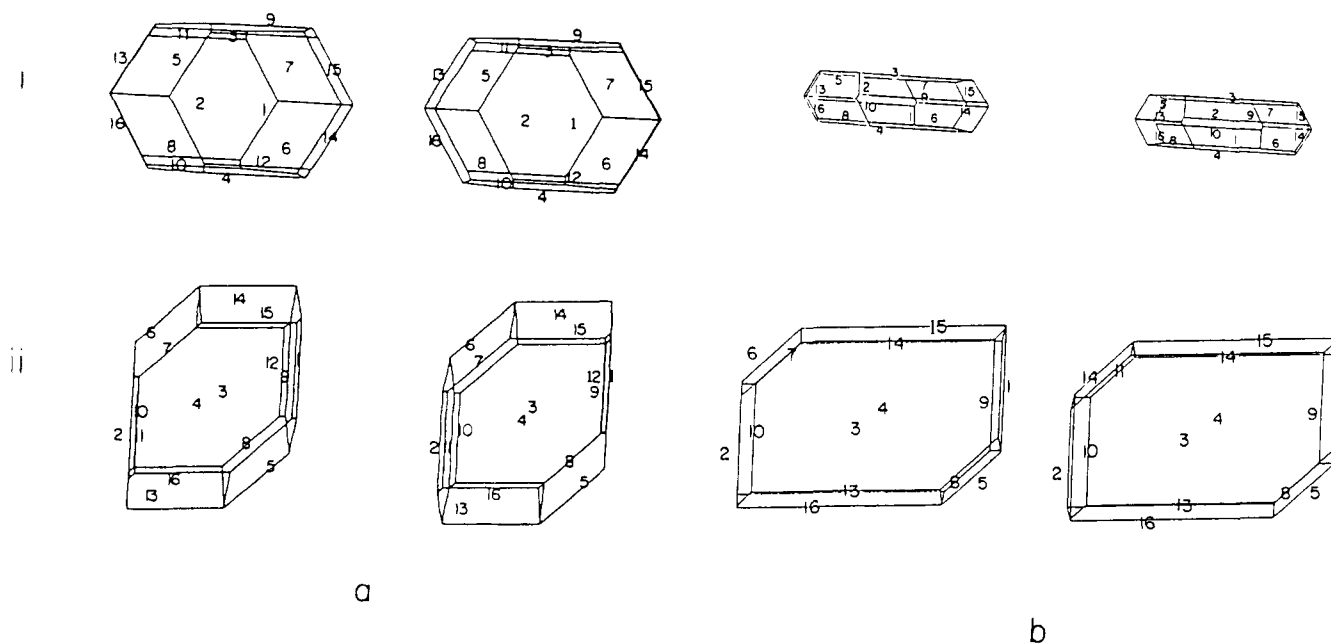


Figure 17. Computer-drawn stereo-pictures of succinic acid crystals as viewed along the *a* and *b* axes (i and ii, respectively): (a) the "theoretical form"; (b) crystals obtained by sublimation. The numbering of the faces: (1) (1,0,0); (2) ($\bar{1}$,0,0); (3) (0,1,0); (4) (0, $\bar{1}$,0); (5) (1,1,1); (6) ($\bar{1}$, $\bar{1}$, $\bar{1}$); (7) ($\bar{1}$,1, $\bar{1}$); (8) (1, $\bar{1}$,1); (9) (1,1,0); (10) ($\bar{1}$, $\bar{1}$,0); (11) ($\bar{1}$,1,0); (12) (1, $\bar{1}$,0); (13) (0,1,1); (14) (0, $\bar{1}$, $\bar{1}$); (15) (0,1, $\bar{1}$); (16) (0, $\bar{1}$,1).

Table X. Succinic Acid: Strongest Intermolecular Interactions (kcal/mol) in the Crystal^a

neighbor ^b			symmetry ^c	<i>E</i>	<i>U</i>	<i>E</i> + <i>U</i>
site						
<i>a</i> ₁	<i>a</i> ₂	<i>a</i> ₃				
1	0	-1	1	-3.38	-1.84	-5.22
-1	0	1	1			
0	0	0	2	-1.49	-2.31	-3.80
0	-1	-1	2			
0	-1	0	2			
0	0	-1	2			
-1	0	0	1	0.22	-3.62	-3.40
1	0	0	1			

^a*E* = electrostatic energy; *U* = van der Waals energy. ^bSee Table II. ^c(1) *x*, *y*, *z*; (2) $-x$, $1/2 + y$, $1/2 - z$.

Table XI. Succinic Acid: Layer Energy (*E*_l, kcal/mol) and Attachment Energy (*E*_{att}, kcal/mol) of Various Low-Index Faces Arranged in Decreasing Order of Their *E*_l

face	<i>E</i> _l	<i>E</i> _{att}	face	<i>E</i> _l	<i>E</i> _{att}
{100}	-24.12	-13.90	{110}	-16.88	-17.52
{020} ^a	-27.24	-12.34	{202} ^a	-12.64	-19.64
{111}	-21.86	-15.03	{111}	-10.11	-20.90
{021}	-18.39	-16.77	{002} ^a	-7.78	-22.07
{011}	-17.46	-17.23			

^aSee Table III.

hydrogen bonds along the *b* axis to form the commonly observed ribbon motif. The ribbons are interleaved along the *c* axis, generating centrosymmetric pairs making close contacts of approximately 4 Å between the centers of the two double bonds (Figure 9).

The intermolecular interactions between a cinnamide molecule and 470 molecules in the crystal were calculated. The strongest of these interactions are listed in Table VIII. *E*_l and *E*_{att} of various low-index faces, calculated using these interactions, are presented in Table IX. There are two alternative ways to define the {002} and {102} layers in (*E*)-cinnamide crystal (Figure 9a, Table IX). The more stable (which grows slower) of each layer was taken to represent the growth rate normal to the respective face.

The "theoretical form" of (*E*)-cinnamide is shown in Figure 10a. Its habit is in agreement with the habit of crystals obtained by sublimation (Figure 10b), but for the small {104} faces which do not appear in the "theoretical form" despite their large calculated M.I. (Table IX).

To derive the habits of (*E*)-cinnamide crystals grown from solution, we analyzed the structure and polarity of several of its real and virtual faces. Electrostatic potential maps of various faces are displayed in Figure 11. Edge-on views of some of the layers are indicated in Figure 9. From the electrostatic maps and the rms of the positive and negative potential values (Figure 11) we deduced the following order of decreasing polarity of the faces of (*E*)-cinnamide:

$$\{011\} \gg \{10\bar{2}\} > \{102\} > \{100\} > \{001\}$$

{011} are the most polar faces, {001} are the least, and the other faces are of intermediate polarity. It was thus predicted that crystals grown from water will have relatively large {011} faces, while in crystals grown from nonpolar solvents, the M.I. of {001} should be enhanced. Figure 12 presents crystals of (*E*)-cinnamide grown from water, ethyl acetate, and benzene, respectively. The habits of the crystals from water and from benzene are in excellent agreement with prediction. Crystals obtained from ethyl acetate exhibit both the polar and nonpolar faces, indicating that ethyl acetate, a solvent of intermediate polarity, affects both polar and nonpolar faces.

Figure 13 displays the M.I., derived from the surface areas of various faces in the crystals obtained from the vapor (sublimation),

(41) (a) Leiserowitz, L.; Schmidt, G. M. *J. Chem. Soc. A* **1969**, 2372-2382. (b) Wang, J. L., unpublished results.

water, ethyl acetate, and benzene. As expected the M.I. of {001} decreases in polar solvents, and increases in nonpolar solvents, while that of {011} increases with the polarity of the solvent.

To support our interpretation of the solvent effect on (*E*)-cinnamide crystal habit, we simulated the habit of (*E*)-cinnamide crystals, grown from polar solvents by modifying the growth rate, represented by *E*_{att}, of the most polar faces {011} in a stepwise manner, while the *E*_{att} of the other faces were kept at their calculated values (Table VIII). Figure 14 demonstrates the gradual change in habit from the sublimation form (Figure 10b) to that of the crystals grown from aqueous solution, as a function of the reduced growth rate normal to the {011} faces. The habits in Figure 14c,d are in good agreement with observation (Figure 12a). In a similar way we simulated the effect of nonpolar solvents by decreasing the growth rate of {001}, keeping the rates of all other faces fixed. The resulting habit (Figure 15d) agrees with that of (*E*)-cinnamide crystals grown from benzene (Figure 12c).

3.5. Succinic acid crystallizes in space group *P2*₁/*c* (*a* = 5.52, *b* = 8.86, *c* = 5.10 Å; β = 91.6°). In succinic acid crystal⁴² planar acid molecules are interlinked by translation along the (011) direction to form chains of H-bonded dimers. The chains are interlinked by CH...O interactions along the glide plane (Figure 16).

The most important of the 160 calculated intermolecular interactions are listed in Table X. *E*_l and *E*_{att} of various low-index faces, arranged in decreasing order of their M.I., are shown in Table XI. The "theoretical form" derived from the calculated *E*_{att} is shown in Figure 17a. The M.I. of the faces of the "theoretical form", derived from their surface areas, fall in the order:

$$\text{M.I.}\{010\} > \text{M.I.}\{100\} > \text{M.I.}\{011\} > \text{M.I.}\{111\} > \text{M.I.}\{110\}$$

Crystals of succinic acid obtained by sublimation (Figure 17b) are very fragile with prominent {010} faces and side faces identical with those predicted by calculation. Thus the agreement between the calculated and observed forms is good though there are minor differences in shape (Figure 17a,b).

To account for the effect of solvent on succinic acid crystals,⁴³ we analyzed the structure and polarity of various faces. Electrostatic potential maps of some faces are presented in Figure 18. From these maps and the calculated rms of the positive and negative potential values, the following order of decreasing polarity of succinic acid faces was deduced:

$$\{011\} > \{100\} > \{111\} > \{110\} > \{010\}$$

The polarities of the various faces may be explained in terms of their structures (Figure 16). Carboxylic oxygen and hydrogen atoms project normal to {011} and {100} and thus are easily accessed by polar solvent molecules. On the {010} face there are both hydrophobic sites, where CH groups project normal to the face, and hydrophilic sites, at which carboxyl oxygen atoms are exposed. Consequently, it was predicted that the M.I. of {011}, {100}, and {111} will increase with the polarity of the solvent, while that of {010} will decrease. This prediction is in nice agreement with the observed habits of succinic acid grown from water, ethanol, and 2-propanol (Figures 19 and 20). Crystals of succinic acid from nonpolar solvents, benzene or toluene, appeared as long very thin and fragile needles, which could not be isolated and characterized.

4. Discussion

Intermolecular interactions between molecules in the crystal play a key role in determining crystal growth and shape. We have demonstrated in this paper how these interactions may be exploited for the derivation of crystal morphology. We have outlined a

(42) (a) Broadley, J. S.; Cruickshank, D. W. J.; Morrison, J. D.; Robertson, J. M.; Shearer, H. M. M. *Proc. R. Soc. London, Ser. A* **1959**, 251, 441. (b) Levlie, J. P.; Auvert, G.; Savariault, J. M. *Acta Crystallogr., Sect. B* **1981**, 37, 2185-2189. (c) We used the unit cell of the recent publication,^{42b} in which the two axes *a* and *c* were interchanged relative to the earlier study.^{42a}

(43) Solvent effect on succinic acid crystals was previously studied by Davey et al.^{16c}

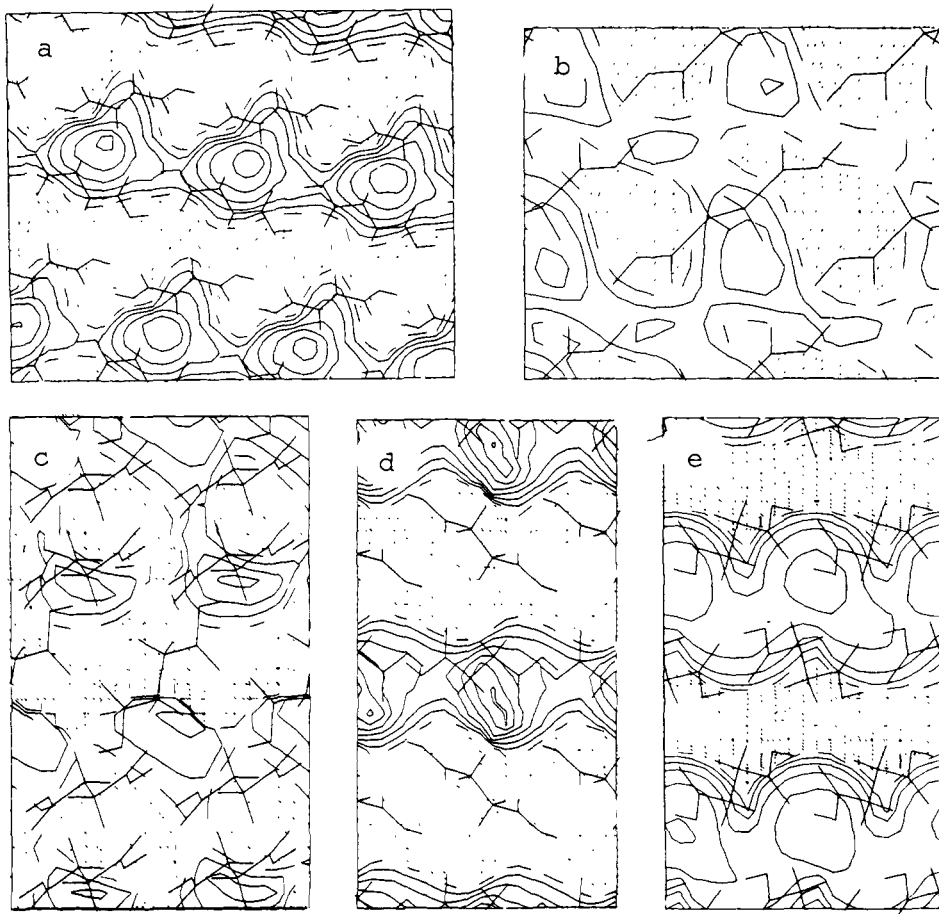


Figure 18. Electrostatic potential maps at closest approach distance to various faces of succinic acid crystals. Molecules belonging to the layers are projected on the potential maps. Solid lines represent repulsive and dotted lines attractive interactions. Contour interval 2 kcal/mol. The rms (in kcal/mol) of the negative and positive values are given in parentheses: (a) {111} (-3.2, 2.7); (b) {010} (-2.0, 1.4); (c) {110} (-3.4, 1.5); (d) {011} (-6.1, 3.5); and (e) {100} (-5.3, 3.2).

method for the derivation of the habit of organic crystals from their internal structure and symmetry. The method has been successfully applied to the crystal habits of a number of organic molecules, α -glycine, (*E*)-cinnamide, succinic acid, benzamide, benzoic acid, glycylglycine³⁴, (*R,S*)-serine,^{18b} androsterone, and succindiamide.⁴⁴ The intermolecular interactions in the crystals, estimated via atom-atom potential-energy calculations, were used for the calculation of layer energy and attachment energy of various low-index crystal faces. From the calculated E_1 it is possible to identify the stable faces, some real and others virtual, which may appear in the growth form when their growth rate is somewhat reduced. For example, {011} of α -glycine were not observed in crystals grown from sublimation but are the most prominent faces in crystals grown from aqueous solution. Similarly, the {100} faces of α -glycine were observed neither in crystals grown by sublimation nor in crystals obtained from aqueous solution, but were reported to be, together with $\{10\bar{1}\}$, the best developed faces in α -glycine crystals crystallized in the presence of NaCl.⁴⁵

The "theoretical form" of crystals obtained using E_{att} as a measure of the growth rate normal to the various faces, is in good agreement with the habits of crystals obtained by sublimation. From the results of this study and other published calculations of crystal habit,¹²⁻¹⁴ which demonstrate a good agreement between observed morphologies and those predicted from the internal structure, it may be concluded that for crystals grown in low supersaturations, the influence of kinetical problems during the crystallization process on the morphology of the crystal is probably the smallest.^{13b}

4.1. Solvent Effect. For solution grown crystals the effect of solvent-solute intermolecular interactions at the various crystal/solution interfaces have a pronounced effect on crystal morphology. When these are strong the solute molecules are solvated, and the growing surfaces of the crystals are covered by solvation layers which must be removed prior to the deposition of additional layers. The degree of solvation, which is determined by the structure of the surface layer, may vary from one face to another. According to accepted theories of crystal growth,^{16a,46} the first stage in the crystallization process is the desolvation of both the crystallizing molecules and the surface site and the entrance of the solute molecule into the solvation layer of the faces. This is followed by surface migration until a step is reached permitting incorporation into the crystal lattice at a kink site. The activation free energies associated with these respective steps are ΔG_{des} , ΔG_{diff} , and ΔG_k . ΔG_{des} and ΔG_{diff} are both dependent on the interactions between the solute and solvent molecules. All three free energies are different on different faces. For growth from the vapor phase $\Delta G_{des} = 0$ and the rate-determining step for growth is ΔG_k . However, for growth from solution, strong interactions between solute and solvent at specific crystal faces may lead to $\Delta G_{des} > \Delta G_k$, and thus the desolvation of specific crystal faces becomes the rate-determining step, with the general effect that the rate of growth of those faces which interact with the solvent is reduced and their M.I.'s are increased.

An alternative way to explain the effect of solvent on crystal habit is through its effect on the surface perfection and on the growth mechanism.¹⁶ According to this approach, favorable interactions between the solute and solvent at specific faces may significantly reduce the interfacial tension and cause a transition

(44) Berkovitch-Yellin, Z., unpublished results.

(45) Fenimore, C. P.; Thrailkill, A. *J. Am. Chem. Soc.* **1949**, *71*, 2714-2717.

(46) Bennema, P. *J. Cryst. Growth* **1967**, *1*, 278-286.

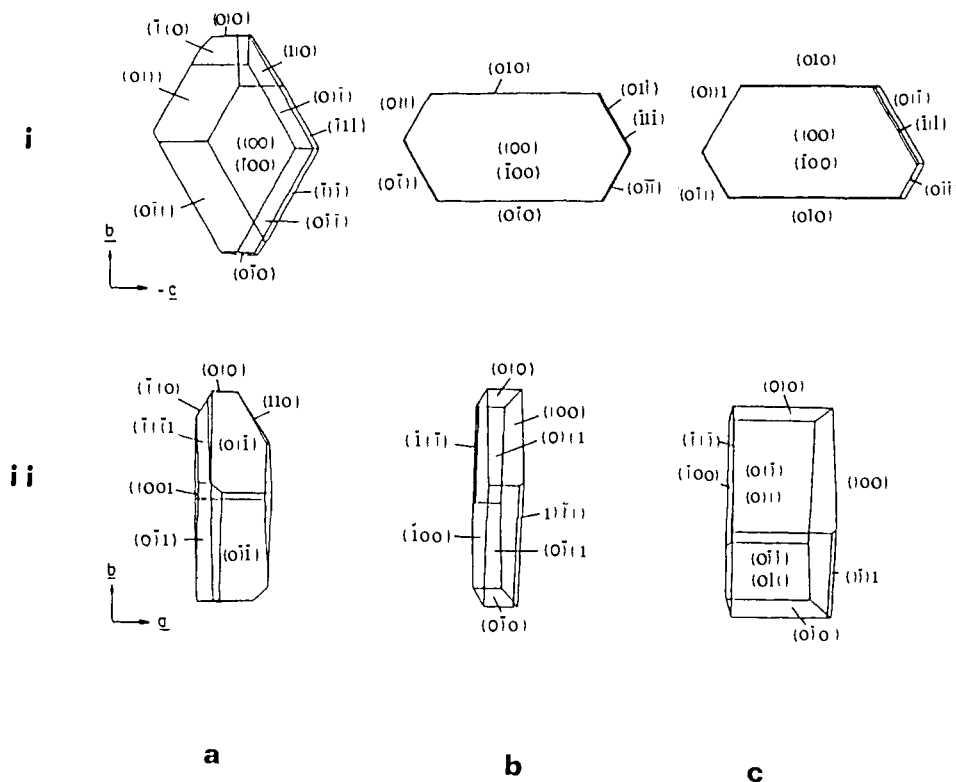


Figure 19. Computer-drawn pictures of succinic acid crystals obtained from solutions of various solvents, as viewed along the *a* and *c* axes (i and ii, respectively): (a) from aqueous solution; (b) from ethanol; (c) from 2-propanol.

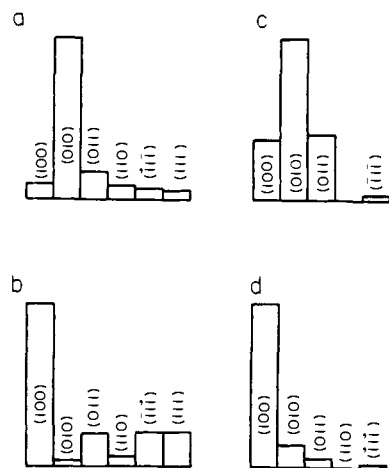


Figure 20. The M.I. of various faces of succinic acid crystals: (a) obtained by sublimation; (b) grown from aqueous solution; (c) grown from 2-propanol; (d) grown from ethanol.

from a smooth to a rough interface. Consequently, the growth kinetics may change from a layer to continuous growth kinetics, the rate of growth of the faces which interact strongly with the solvent is enhanced, and their M.I.'s are reduced. At low supersaturations these two models differ appreciably in their predictions so that experimental results, such as detailed measurements of growth rates, or crystal morphologies may help to discriminate between the two.

In this paper we analyzed the effect of the solvent by comparing the morphologies of crystals grown from different solvents. Another approach that we undertook for elucidating this effect was the study of solvent effect on the growth of polar crystals.⁴⁷ Polar crystals are ideal for such a study because an observed difference between the growth rates of two opposite faces (hkl) and ($\bar{h}\bar{k}\bar{l}$), along a polar direction, originates primarily from

solvent/surface interactions. It was long since observed that the polar crystal of α -resorcinol (space group $Pna2_1$) grows from aqueous solution unidirectionally along the *c* axis; however, the preferred direction of growth is still a matter of debate.^{48,49} The crystals exhibit "benzene-rich" faces at one end of the polar *c* axis and O(hydroxyl)-rich faces at the other end. In 1949 Wells⁴⁸ deduced that the crystal grows preferentially along the direction of the benzene-rich faces, assuming retardation of growth of the O(hydroxyl) faces by the adsorbed water molecules. It was alternatively proposed⁴⁹ that growth is along the O(hydroxyl) direction, assuming that strong solvent/solute interactions at these faces enhance their growth. Recently we have determined the absolute configuration of specimen crystals of α -resorcinol by the Bijvoet method⁵⁰ and by the assistance of "tailor-made" additives,² and established that the growth is along the O(hydroxyl)-rich faces.⁵¹ We have also demonstrated that the benzene-rich faces are acidic and deduced that because of their structure these faces bind the solvent stronger than the O(hydroxyl)-rich faces. This deduction is now being studied by energy calculations.

From the results presented in this paper, the case of α -resorcinol, and the analysis of other published results on the effect of solvent on crystal habit,^{13,16} we are inclined to the view that the most important effect of solvent on the habits of crystals grown at low supersaturation originates from inhibition of the growth of those faces which interact with the solvent most strongly. Thus in those cases where there are large differences in the solvent/solute intermolecular interactions at the various crystal faces, large solvent effects are anticipated, due to the change in the relative growth rates of crystal faces. Crystals obtained from polar solvents exhibit relatively large polar faces, while nonpolar faces are enhanced in crystals which are grown in nonpolar solvents. Crystals which are obtained from solvents of intermediate polarity exhibit both

(48) Wells, A. F. *Discuss. Faraday Soc.* **1949**, *5*, 197.

(49) Milisavljevic, Thesis, E.T.H., Zurich, Diss. N6898.

(50) Bijvoet, J. M.; Peerdeman, A. F.; van Bommel, A. J. *Nature (London)* **1951**, *168*, 271.

(51) (a) Wireko, F. C.; Berkovitch-Yellin, Z.; Frolow, F.; Lahav, M. and Leiserowitz, L., unpublished results. (b) Wireko, F. C. M.Sc. Thesis, submitted to the Feinberg Graduate School, Weizmann Institute of Science, Rehovot, Israel, 1985.

(47) The word polar in this context indicates that all molecules are aligned in the same direction in the crystal vis-à-vis the polar axis.

polar and nonpolar faces to different extents. We have found that if the relative polarities of the various crystal faces are known, it is possible to predict the habit modification induced by a solvent of a specific nature in those systems where there are large differences in the polarity of the faces. We have demonstrated that electrostatic potential maps at closest approach distances to the various crystal faces are instructive for the study of the polarities of crystal faces. However, to understand the detailed differences

between faces of comparable nature, it is necessary to calculate the binding energy of the solvent molecules to the various faces. Studies on this line are presently underway.⁵¹

Acknowledgment. The author thanks E. Gati for her devotion in growing the crystals, L. Addadi, L. Leiserowitz, and M. Lahav for useful discussions, and F. Hirshfeld for a critical reading of the manuscript.

Communications to the Editor

Specific Rate Enhancement by Olefin Coordination in Reductive Elimination of η^3 -Allylpalladium Complexes

Hideo Kurosawa,* Mitsuhiro Emoto, Akira Urabe, Kunio Miki, and Nobutami Kasai*

Department of Applied Chemistry, Osaka University
Suita, Osaka, Japan

Received August 1, 1985

Increasing attention has been paid to reductive elimination of allylmetal complexes as a key step in organic synthesis.¹⁻³ Of particular help in raising the synthetic value of the reaction of allylpalladium complexes was the unique use of some olefinic additives (e.g., maleic anhydride) not as a substrate but a mediator.¹ We wish to report on mechanistic studies of the reaction of both η^3 - and η^1 -allylpalladium complexes with some olefins which shed light on the origin of such unique role of the olefinic additives.

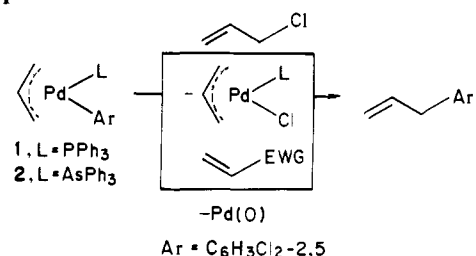
We found previously⁴ that reductive elimination of η^3 -allyl complex **1** is greatly accelerated by some olefins (e.g., allyl chloride, maleic anhydride) (Scheme I). . . Notably, this reaction was retarded considerably by addition of free PPh₃. Now kinetics of the reaction of **2**⁵ in toluene at 0 °C could be followed cleanly⁶ in the presence of added AsPh₃ [(2.2 × 10⁻⁴) - (2.2 × 10⁻³) M for the reaction of allyl chloride; 0.02-0.4 M for other olefins⁷]. Under the pseudo-first-order condition ([**2**] = 0.005-0.02 M, [olefin] = 0.05-2.46 M), the rate obeyed⁸ eq 1 for the reaction

$$\text{rate} = k_{\text{obsd}}[\mathbf{2}] = [k_1[\text{olefin}]/(k_2 + [\text{AsPh}_3])][\mathbf{2}] \quad (1)$$

$$\text{rate} = k_{\text{obsd}}[\mathbf{2}] = [k_1[\text{olefin}]/[\text{AsPh}_3]][\mathbf{2}] \quad (2)$$

of C₃H₅Cl and (E)-CNCH=CHCN or eq 2 for the rest.⁷ In Table I are summarized the rate data for several olefins. Styrene

Scheme I



Scheme II

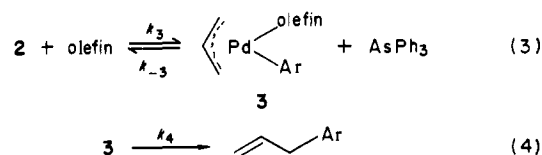


Table I. Rate Data^a for Some Olefins

olefin	k_1, h^{-1}
CH ₂ =CHCH ₂ Cl ^b	2.0 × 10 ⁻⁴
CH ₂ =CHCN	2.5 × 10 ⁻³
CH ₂ =CHCOOMe	4.5 × 10 ⁻³
(Z)-MeOOCCH=CHCOOMe	1.5 × 10 ⁻²
(E)-MeOOCCH=CHCOOMe	0.24
(E)-NCCH=CHCN ^c	0.44

^aIn toluene at 0 °C. For rate expression, see eq 1 and 2. ^b $k_2 = 1.7 \times 10^{-4} \text{ M}$. ^c $k_2 = 8.0 \times 10^{-2} \text{ M}$.

and allylbenzene were not reactive enough to give accurate k_1 values.

A most probable pathway consistent with eq 1 is shown in Scheme II⁹ where a steady-state approximation is applied to the intermediate **3** ($k_1 = k_3k_4/k_{-3}$, $k_2 = k_4/k_{-3}$). It may well be that in **3** allyl chloride is coordinated with Pd through the C=C bond, and oxidative addition of this substrate¹⁰ is included in eq 4. This is supported by the observation that addition of CH₂=CMeCH₂Cl to a mixture of **2**/AsPh₃ did not lead to the formation of C-H₂=CHCH₂Cl. It seems also reasonable to assume [AsPh₃] >> k_4/k_{-3} under the conditions employed for obtaining eq 2.⁷

The trend of k_1 ($=k_3k_4/k_{-3}$) (Table I) in the main reflects the order of the electrophilic nature of the olefin.¹⁰ Although we could

(9) Formation of no adducts between **2** and AsPh₃, as revealed by ¹H NMR spectra, strongly suggests that inverse dependence of the rate on [AsPh₃] is attributable to inhibition of a dissociative path. An alternative to Scheme II would be a rapid preequilibrium to form Pd(η^3 -C₃H₅)(Ar) and free AsPh₃ (K_{eq}), followed by a slow reaction of this intermediate with the olefin (k_3), also giving rise to eq 1 ($k_1 = k_3K_{\text{eq}}$, $k_2 = K_{\text{eq}}$). However, this can be excluded in view of the great difference of the k_2 values for C₃H₅Cl and (E)-NCCH=CHCN (see Table I).

(10) The higher electrophilicity of (E)- than (Z)-MeOOCCH=CHCOOMe was reported; Glass, R. S.; McConnell, W. W. *Organometallics* 1984, 3, 1630. See also Yamamoto, T.; Yamamoto, A.; Ikeda, S. *J. Am. Chem. Soc.* 1971, 93, 3350.

(1) (a) Goliaszewski, A.; Schwartz, J. *Organometallics* 1985, 4, 415. (b) *Ibid.* 1985, 4, 417. (c) *J. Am. Chem. Soc.* 1984, 106, 5028. (d) Temple, J. S.; Riediker, M.; Schwartz, J. *Ibid.* 1982, 104, 1310. (e) Hayasi, Y.; Riediker, M.; Temple, J. S.; Schwartz, J. *Tetrahedron Lett.* 1981, 22, 2629.

(2) (a) Sheffy, F. K.; Godschalx, J. P.; Stille, J. K. *J. Am. Chem. Soc.* 1984, 106, 4833. (b) Matsushita, H.; Negishi, E. *Ibid.* 1981, 103, 2882. (c) Hayashi, T.; Konishi, M.; Yokota, K.; Kumada, M. *J. Chem. Soc., Chem. Commun.* 1981, 313. (d) Consiglio, G.; Morandini, F.; Piccolo, O. *Ibid.* 1983, 112.

(3) Keim, W.; Behr, A.; Röper, M. "Comprehensive Organometallic Chemistry"; Wilkinson, G.; Stone, F. G. A., Eds.; Pergamon Press: Oxford, 1982; Chapter 52.

(4) (a) Kurosawa, H.; Emoto, M.; Urabe, A. *J. Chem. Soc., Chem. Commun.* 1984, 968. (b) Numata, S.; Kurosawa, H. *J. Organomet. Chem.* 1977, 131, 301.

(5) Kurosawa, H.; Emoto, M. *Chem. Lett.* 1985, 1161.

(6) All kinetic runs in this work were carried out similarly to those reported.^{4a,5}

(7) Kinetic measurements at the lower concentrations of AsPh₃ were hampered by less satisfactory first-order dependence of the rate on [**2**] under these conditions.

(8) Conventional plots of k_{obsd} vs. [olefin] gave straight lines passing through the origin. Plots of $1/k_{\text{obsd}}$ vs. [AsPh₃] were also linear, but meaningfully large intercepts could be evaluated only in the reaction of C₃H₅Cl and (E)-NCCH=CHCN.